

1           **Physical characteristics of kimberlite and basaltic intraplate volcanism, and**  
2                           **implications of a biased kimberlite record**

3  
4                           Richard J. Brown<sup>1</sup> and Greg A. Valentine<sup>2</sup>

5  
6                           <sup>1</sup>Department of Earth Sciences, Durham University, Durham, DH1 3LE, UK

7   email: Richard.brown3@durham.ac.uk

8                           <sup>2</sup>Department of Geology, 411 Cooke Hall, University at Buffalo, Buffalo, NY14260 USA

9   email: gav4@buffalo.edu  
10

11   **Abstract**

12   Bias in the record of kimberlite volcanism is assessed by using newly acquired size data on >900  
13   kimberlite bodies from 12 kimberlite fields eroded to depths of between 0–>1200 m, and by a  
14   comparison with intraplate monogenetic basaltic volcanic fields. Eroded kimberlite fields are  
15   composed of pipes (or diatremes) and dikes and within any one kimberlite field, regardless of erosion  
16   level, kimberlite bodies vary in area at the Earth’s surface over 2–3 orders of magnitude. Typically 60–  
17   70% of the bodies are <10% the area of the largest pipe in the field. The maximum size of a kimberlite  
18   pipe found in a field shows a relationship with estimated erosion levels suggesting that the erosion  
19   level of a region could be used to predict the maximum potential size of a pipe where it intersects the  
20   surface. The data indicate that the selective removal of surface volcanic structures and deposits by  
21   erosion has distorted the geological record of kimberlite volcanism. Selective mining of preferentially  
22   large, diamondiferous kimberlite pipes and underreporting of small kimberlite pipes and dikes adds  
23   further bias. A comparison of kimberlite volcanic fields with intraplate monogenetic basaltic volcanic  
24   fields indicates that both types of volcanism overlap in terms of field size, volcano number and size,  
25   and typical erupted volumes. Eroded monogenetic basaltic fields comprise dikes that fed effusive and  
26   weakly explosive surface eruptions, and diatremes (pipes) generated during phreatomagmatic  
27   eruptions, and are structurally similar to eroded kimberlite fields. Reassessment of published data  
28   suggests that kimberlite magmas can erupt in a variety of ways and that most published data, taken  
29   from the largest kimberlite pipes, may not be representative of kimberlite volcanism as a whole. This  
30   refuels long-standing debates as to whether kimberlite pipes (diatremes) primarily result from  
31   phreatomagmatic eruptions (as in basaltic volcanism), or from volatile-driven magmatic eruptions.  
32

33 **Keywords:** kimberlite; basalt; monogenetic volcanism; erosion; diatreme; phreatomagmatism

34

## 35 **Introduction**

36 All forms of terrestrial volcanism result in the eruption of material onto the Earth's surface and  
37 the emplacement of magma and debris in the shallow to deep subsurface. Post-volcanic erosion can  
38 expose the subsurface features. The proportions of erupted volume relative to the volume of the  
39 shallow subsurface plumbing (or feeder) structure of a monogenetic volcano vary between different  
40 eruption styles. Most of the mass of a magmatic (meaning, driven dominantly by expansion of  
41 magmatic volatiles) basaltic eruption is emplaced on the Earth's surface as lava or pyroclastic cones;  
42 their feeder systems merge downward to narrow dikes within ~200 m below the surface (Keating et al.,  
43 2008; Valentine, 2012), and thus have small volumes. In contrast, explosive phreatomagmatic (where  
44 magma fragmentation is strongly influenced by explosive magma-water interaction) maar-forming  
45 eruptions produce surface tephra deposits, and in the subsurface produce deep, wide diatremes that may  
46 have volumes similar to or even larger than the erupted volumes. This results from extensive disruption  
47 of country rocks from repeated subterranean explosions, intrusion of magma bodies, and explosion-  
48 driven churning and subsidence of material (e.g., Lorenz, 1975; Lorenz and Kurszlaukis, 2007; White  
49 and Ross, 2011; Valentine and White, 2012). Landscape erosion can introduce bias into the geological  
50 record by removing surface and shallow-level rocks whilst preserving subsurface intrusions, conduits  
51 and diatremes. This should apply to kimberlite volcanism, occurring episodically for >1 Ga, in the  
52 same manner as it does for all other types of volcanism. Kimberlite eruptions have not been witnessed,  
53 surface volcanic deposits and edifices are extremely scarce, and much remains unknown about the  
54 behavior of these magmas at the Earth's surface. At the last count, approximately 5000 kimberlite  
55 bodies had been documented worldwide (Kjarsgaard, 1996). Most of these are pipes (diatremes filled  
56 predominantly with kimberlitic juvenile material and fragmented country rock) or dikes emplaced into  
57 stable cratonic crust subject to low rates of erosion (e.g., 10–15 m/Ma, Hanson et al., 2009). The effects  
58 of landscape erosion are significant due to the great age of many kimberlites—almost all known  
59 kimberlites are Eocene or older. Early models for kimberlite volcanism were strongly influenced by  
60 deposits and features of heavily eroded pipes (e.g., Hawthorne, 1975). Current understanding of  
61 kimberlite volcanoes is strongly biased because most data have been derived from large subsurface  
62 mined kimberlite pipes that have experienced at least several hundred meters of post-emplacement  
63 erosion and have lost their upper parts from the geological record (see reviews in Nixon, 1995; Field  
64 and Scott Smith, 1999; Field et al., 2008).

65           In this paper, we ask: how representative is the information gathered from studied kimberlite  
66 pipes? What has been the effect of erosion in biasing the record of kimberlite volcanism—what  
67 evidence, deposits and structures may have been preferentially removed or emphasized by erosion from  
68 kimberlite volcanic fields? We address these questions through a cautious interrogation of size data on  
69 >900 kimberlite bodies from 12 kimberlite fields that are thought to have been eroded to various  
70 depths, and through comparison with intraplate basaltic volcanic fields which are kimberlites' closest  
71 cousins in terms of volume, tectonic setting, and magma composition (note: we include volcanic  
72 systems that commonly are, in detail, alkali basaltic or ultramafic in composition). The latter suggests  
73 that intraplate basaltic volcanic fields and their eruptions can offer close analogy to some major aspects  
74 of kimberlite volcanism, allowing for differences in detail due to magma properties. Analysis of size  
75 data from kimberlite fields suggests that the apparent predominance of large pipe structures in many  
76 kimberlite fields may result from bias in the geologic record, the selection of mining sites, and  
77 underreporting of smaller bodies (dikes and small or shallow volcanic conduits). We argue that the  
78 latter are more common than previously recognized, suggesting that large kimberlite pipes represent  
79 only a fraction of kimberlite volcanism rather than being representative of it. The apparent dominance  
80 of kimberlite pipes in kimberlite fields may have contributed to a misperception that a  
81 phreatomagmatic model for the formation of kimberlite pipes (e.g., Lorenz, 1975; Lorenz and  
82 Kurszlauskis, 2007; White and Ross, 2011) would seem to require all kimberlite magmas to erupt  
83 phreatomagmatically, and in turn, has led researchers to focus on magmatically-driven processes to  
84 explain features present in kimberlite pipes (e.g., Hawthorne, 1975; Skinner and Marsh, 2004; Sparks  
85 et al., 2006; Wilson and Head, 2007; Cas et al., 2008; Porritt et al., 2008; Brown et al., 2009). The  
86 presented data and observations in this paper refuel this debate. The results are of broad interest to  
87 those investigating the nature of monogenetic basic and ultrabasic volcanism, intrusive igneous  
88 processes in the near-surface, and to geoscientists involved in diamond exploration and mining. The  
89 study feeds into investigations of the rates of landscape erosion in continental interiors.

90

## 91 **Review of physical geology of kimberlites**

### 92 *Geologic settings, temporal and spatial patterns*

93           Kimberlite pipes, dikes and sills are found on all continents and most are confined to the  
94 ancient cratonic regions. They span the early Proterozoic through to the Eocene in age, but worldwide  
95 show marked clustering through time. Peaks in kimberlite activity follow major plate re-organizations  
96 and coincide with variations in direction and/or in speed in plate motion, and to uplift and erosion

97 relating to episodic tectonic instability and large igneous province (LIP) formation (e.g., Marsh, 1973;  
98 Jelsma et al., 2004; Snyder and Lockhart, 2005; Moore et al., 2008; Jelsma et al., 2009).

99         Kimberlites occur in fields (or clusters) that cover hundreds to thousands of square kilometers  
100 and contain up to several hundred kimberlite bodies. There is a long-recognized relationship between  
101 crustal structure and the distribution of kimberlites and kimberlite fields (Marsh, 1973; Haggerty, 1982,  
102 White et al., 1995; Vearncombe and Vearncombe, 2002). Some linear fields parallel geophysical  
103 anomalies in the mantle lithosphere (Snyder and Lockhart, 2005) and some are associated with deep,  
104 transcontinental crustal fractures or shear zones (“cryptic corridors” of Jelsma et al., 2004). Smaller  
105 scale structures control the distribution of kimberlite bodies within fields (Jelsma et al., 2004) and the  
106 shapes of pipes (Kurszlaukis and Barnett, 2003; Lorenz and Kurszlaukis, 2007). Individual pipes may  
107 be situated at the intersection of major fractures or faults (Dawson 1970; Kurszlaukis and Barnett,  
108 2003).

109

#### 110 *Dikes*

111         There are few detailed studies of kimberlite dikes and sills (Dawson and Hawthorne, 1973;  
112 Gurney and Kirkley, 1996; Basson and Viola, 2003; Brown et al., 2007; Kavanagh and Sparks, 2011;  
113 Gernon et al., 2012; White et al., 2012). Kimberlite dikes occur in regional swarms (Nixon, 1973;  
114 Kresten and Dempster, 1973). They are commonly exposed at the same level as large kimberlite pipes  
115 in many fields (e.g., Moss, et al., 2009) and occur as late-stage intrusions within pipes (Kurszlaukis and  
116 Barnett, 2003). All kimberlite pipes are rooted in dikes. Kimberlite dikes are between 0.03–8 m wide  
117 with mean dike thicknesses of ~0.5 m (e.g., Nixon, 1973; Rombouts, 1987; Kavanagh and Sparks,  
118 2011). Dikes can form en echelon segments (Basson and Viola, 2003) and are continuous over  
119 distances of up to 0.5–10 km, but are probably much longer at depth (Snyder and Lockhart, 2005). We  
120 suspect that kimberlite dikes and sills are under-reported within most kimberlite fields due to their poor  
121 exposure, small size and mostly poor economic potential, even though they adjacent to most mined  
122 kimberlite pipes. It is interesting that numerous kimberlite dikes have been documented in well-  
123 exposed regions (e.g., Lesotho; Nixon, 1973).

124

#### 125 *Kimberlite pipes*

126         Kimberlites pipes are downward-tapering volcanic conduits with upper diameters that may  
127 exceed 500 m. They can reach >2 km deep and have volumes of  $10^6$ – $10^8$  m<sup>3</sup> (e.g., Clement, 1982;  
128 Nixon, 1995; Field and Scott Smith, 1999; Field et al., 2008). The walls of kimberlite pipes generally  
129 dip inward at steep angles (~80–85°) but may dip at shallower angles, and be vertical or slightly

130 outward-dipping over scales of tens to hundreds of meters. Dip angles in the near surface may be  
131 shallower due to cutting through weak sediment layers and through neighboring pipes (e.g., Field et al.,  
132 1997; Kurszlaukis et al., 2009). In cross-section (map view) they are roughly circular to ellipsoidal and  
133 may become more irregularly shaped downward. The orientation of joints and faults in the country  
134 rock and the regional stress field can influence the shape of pipes (e.g., Barnett, 2008). Lower parts of  
135 kimberlite pipes (root zones, e.g., Clement, 1982) transition into dikes.

136 Kimberlite pipes are filled with a variety of rocks and no two kimberlite pipes are exactly alike  
137 (see Field and Scott Smith, 1999; Sparks et al., 2006; Kjarsgaard, 2007). Most pipes contain rocks  
138 composed of juvenile pyroclasts, phenocrysts, mantle debris and crustal rocks, the latter derived  
139 predominantly from host rocks that occupied the volume of the pipe prior to eruption. Volcaniclastic  
140 rocks within kimberlite pipes can be massive or layered. Layered volcaniclastic kimberlite lithologies  
141 include pyroclastic and sedimentary rocks that exhibit bedding and stratification on different scales and  
142 defined by variations in grainsize and/or composition. Massive volcaniclastic rocks commonly show  
143 evidence for gas fluidization including restricted grainsize distributions, gas escape pipes, and  
144 homogenous mixing of lithic clast types (Walters et al., 2006; Gernon et al., 2008), although the role of  
145 wholesale (versus local, meters to tens of meters scale) fluidization of kimberlite pipes is contentious  
146 (e.g., White and Ross, 2011). Matrix- to clast-supported marginal wall rock breccias occur at many  
147 levels (e.g., Barnett, 2004; Brown et al., 2009). Dikes, sills, bulbous intrusive bodies, lavas and lava  
148 lakes and welded pyroclastic rocks have also been recognized in some pipes (e.g., Brown et al., 2008a).  
149 Rock units and lithofacies within kimberlite pipes are commonly arranged in pseudo-concentric  
150 patterns, forming complex structures that might indicate alternating erosion and filling phases (see  
151 Kjarsgaard, 2007; Field et al., 2008 and references therein; Brown et al., 2009). Kimberlite pipes and  
152 their contained deposits share many structural and geological characteristics with diatremes beneath  
153 maar volcanoes (e.g., Lorenz, 1975; Lorenz and Kurszlaukis, 2007; White and Ross, 2011).

154

### 155 **Sizes of kimberlite volcanoes and their plumbing systems**

156 Much of the data on kimberlite fields is not in the public domain but we have obtained a unique  
157 dataset on the sizes (plan view area) of 912 kimberlite bodies from 12 kimberlite fields in seven  
158 countries (Table 1). The data represent geophysical anomalies detected mostly during aerial magnetic  
159 surveys and field campaigns. The reported kimberlite bodies are variably buried beneath glacial till,  
160 desert sand or soil, or are exposed to varying degrees at the Earth's surface. Cross-section (map view)  
161 shape data for the kimberlite bodies is not available. The size data are reported in square meters and as  
162 diameters derived from the square root of the area. Caution is needed in interpreting the data because

163 the size of a geophysical anomaly can be dependent on lithology (magnetic vs. non-magnetic  
164 lithologies) and because not all anomalies have been confirmed by drilling (or the data are not  
165 available). The sizes of geophysical anomalies in shallowly-eroded kimberlite fields (Table 1) need to  
166 take into account crater flaring and coalescence with neighboring kimberlites. Dikes are less likely to  
167 be detected by geophysical surveys especially when the country rock has a strong magnetic signature.  
168 The amount of erosion is difficult to assess and poorly quantified: erosion estimates have been derived  
169 from several different qualitative lines of evidence (e.g., regional stratigraphic surveys, geological  
170 mapping and the lithic inclusions contained within kimberlite pipes; Hanson et al., 2009). Below we  
171 illustrate the main features of kimberlite fields that are thought to have experienced between 0–1250 m  
172 erosion. We consider that the estimates of erosion may well have errors of  $\pm 200$  m. Nevertheless, we  
173 consider that general trends drawn out of the dataset, which represents 15–20% of known kimberlite  
174 bodies worldwide, are representative enough of kimberlite volcanism to make some valid observations,  
175 tentative interpretations and draw some preliminary conclusions. This is supported by the similarity in  
176 the size distributions of different kimberlite fields.

177

#### 178 *Little eroded kimberlite fields*

179 The only known examples of exposed kimberlite edifices are the three Holocene Igwisi Hills  
180 volcanoes (IHV), Tanzania (Fig. 1; Dawson, 1994; Brown et al., 2012). These are small volcanoes with  
181 erupted volumes of  $>0.001 \text{ km}^3$  (Fig. 1). The NE volcano resembles a small maar volcano with a 200 m  
182 diameter crater at or near the pre-eruptive surface. A 500 m-long lava flow extends away from the NE  
183 of the volcano. The central volcano has a partial tephra cone built up on the NW side of a  $<100$  m  
184 diameter crater filled with a lava coulee (Brown et al., 2012). The SW volcano is a small pyroclastic  
185 cone, with a perched crater,  $<180 \times 100$  m in diameter. Crater surface areas at the pre-eruptive surface  
186 range from  $<7 \times 10^3$  to  $3 \times 10^4 \text{ m}^2$ . The central and SW volcanoes share similarities with basaltic scoria  
187 cones. There is little evidence for substantial excavation of deep conduits beneath the volcanoes and  
188 Brown et al. (2012) concluded that the conduits beneath the central and SW volcanoes were probably  
189 similar in dimensions to those beneath basaltic scoria cones (c.f., Keating et al., 2008; Valentine,  
190 2012).

191 The  $>69$  Cretaceous Fort à la Corne kimberlites (Fig. 2), Canada, are presently buried under  
192 thick glacial till and comprise pyroclastic rocks and reworked volcanoclastic rocks emplaced in a  
193 coastal or submarine environment (e.g., Leckie et al., 1997; Berryman et al., 2004; Pittari et al., 2008).  
194 They have been interpreted as either shallow, wide craters filled with pyroclastic rocks (Berryman et  
195 al., 2004), or positive relief tephra cones and tuff rings (Leckie et al., 1997; Zonneveld et al., 2004;

196 Kjarsgaard, 2007; Harvey et al., 2009), or some combination of the two (Pittari et al. 2008; Lefebvre  
197 and Kurszlaukis, 2008). Conduits have been drilled to depths of 700 m. Seismic reflection surveys of  
198 the kimberlite body 169 outlines a cone 50–100 m high and >1 km in diameter (e.g., Kjarsgaard, 2007).  
199 The near-shore setting has led many authors to infer that the eruptions were in part phreatomagmatic  
200 (Lefebvre and Kurszlaukis, 2008; Pittari et al., 2008; Kjarsgaard et al., 2009). Substantial kimberlite  
201 pipes have not been located beneath the Fort à la Corne kimberlite volcanoes. This may indicate  
202 similarities to basaltic tuff rings and tuff cones where phreatomagmatic explosions were very shallow  
203 or/and dominated by surface water rather than groundwater (see White and Ross, 2011).

204 The Cretaceous Alto Cuilo kimberlite field, Angola, comprises >200 kimberlites buried under  
205 Kalahari sand (Pettit, 2009; Table 1). The kimberlites erupted through Karoo sediments and have been  
206 imaged primarily by airborne magnetic surveys. Kimberlite craters, and in some cases, extra crater  
207 lavas are unusually well preserved (Eley et al., 2008). Shallow geophysical data suggest that some  
208 large craters appear to flare upwards. Geological data are sparse on each target, but some general  
209 statements can be made about the field, based on the size data. Approximately 60% of the kimberlites  
210 are <400 m in diameter ( $1.2 \times 10^5 \text{ m}^2$ ), and approximately 30% are <250 m in diameter ( $1.9 \times 10^5 \text{ m}^2$ , Fig.  
211 3). There is limited information on the nature of the preserved volcanoes: some may represent eroded  
212 craters, while others may still have surface parts of cones preserved. Pettit (2009) considered that they  
213 are comparable to the Fort à la Corne kimberlite volcanoes (Table 1).

214 Other examples of kimberlite volcanoes include the Meso-Neoproterozoic Tokapal kimberlite,  
215 India (Mainkar et al., 2004)—a 2 km wide, 70 m thick buried and eroded tuff ring.

216

### 217 *Shallowly eroded kimberlite fields*

218 The 85 kimberlites of the Cretaceous Orapa kimberlite field, Botswana, are considered to have  
219 experienced <200 m erosion since emplacement (Table 1; Field et al., 1997; Gernon et al., 2009a, b).  
220 The largest kimberlite pipe (A/K1 South) has a flared crater that has cut into the neighboring pipe  
221 (A/K1 North). 98% of the kimberlites are <400 m in diameter ( $1.2 \times 10^5 \text{ m}^2$ ); approximately 47% are  
222 <110 m ( $1.1 \times 10^4 \text{ m}^2$ ) in diameter and 25% are <50 m in diameter ( $2 \times 10^3 \text{ m}^2$ ; Fig. 3). Dikes have been  
223 uncovered by mining operations around the large kimberlite pipes although data are sparse.

224 Cretaceous kimberlites in Northern Lesotho have been subject to ~300 m of erosion (Hanson et  
225 al., 2009) and are exposed over an area  $10 \times 100 \text{ km}$  (Dempster and Tucker, 1973; Kresten and  
226 Dempster, 1973; Nixon, 1973; Jelsma et al., 2009). Due to the mountainous terrain and thin patchy  
227 overburden numerous kimberlite dikes are exposed (Fig. 4). Nixon (1973) reports a dike swarm,  
228 trending  $300^\circ$ , with >220 individual dike segments, 21 blows ~8–40 m wide (or ‘buds’ sensu Delaney

229 and Pollard, 1981, thicker sections along dikes that may contain breccia), and 17 pipes between 70–500  
230 m in diameter ( $1.5 \times 10^4$ – $8 \times 10^5$  m<sup>2</sup>). Pipes contain volcanoclastic rocks. Individual dike segments are  
231 0.1–7 m wide and 50% are continuous over <50 m, although this is controlled largely by exposure.  
232 Some 13% can be traced for over 1 km. The longest extends for >9 km.

233

#### 234 *Moderately eroded kimberlite fields*

235 The 159 Upper Cretaceous to Paleogene Ekati kimberlites, Canada (Table 1) are thought to  
236 have experienced several hundred meters erosion (<500 m; Nowicki et al., 2004). The largest pipe has  
237 a diameter of 450 meters. Approximately 60% are <100 m in diameter; 10% are <60 m in diameter.  
238 Dikes are common adjacent to the pipes (Nowicki et al., 2004).

239 The Cambrian Venetia kimberlite field, South Africa, is considered to have been eroded to  
240 depths of ~500 m and comprises >15 pipes and dikes (Table 1, Kurszlaukis and Barnett, 2003). The  
241 erosion level has been estimated from the presence of Karoo sedimentary rocks in the pipes which have  
242 been eroded from the region. The largest pipe, K1, is irregular, elongate, and is 650×250 m in diameter  
243 ( $1.2 \times 10^5$  m<sup>2</sup>). Eleven of the pipes are <90 m in diameter ( $<6 \times 10^4$  m<sup>2</sup>). Some kimberlite bodies are  
244 dikes (e.g., K8 kimberlite, Kurszlaukis and Barnett, 2003) and late-stage dikes are present within the  
245 large pipes and around them.

246

#### 247 *Deeply eroded kimberlite fields*

248 Two groups of kimberlites outcrop in the Kimberley area, South Africa. A younger group  
249 emplaced around 111–97 Ma, is thought to have experienced ~850 m of erosion (Hanson et al., 2009).  
250 This group comprises 68 kimberlite bodies, the largest of which is 400 m in diameter ( $1.3 \times 10^5$  m<sup>2</sup>, Fig.  
251 3); 42% are <110 m in diameter and 25% are <60 m in diameter.

252 The older group (119–114 Ma) comprises 134 kimberlites that have experienced ~1250 m of  
253 erosion (Hanson et al., 2009). The largest pipe is 270 m in diameter ( $5.5 \times 10^4$  m<sup>2</sup>). 80% are <100 m in  
254 diameter and 35% are less than 40 m in diameter (Fig. 3).

255

#### 256 *General trends*

257 These newly acquired data from kimberlite fields exposed at various paleo-depths allow us to  
258 examine the subsurface plumbing systems of kimberlite fields. The eroded kimberlite fields are  
259 composed of pipes and dikes, but the data do not allow distinction between dikes and small pipes  
260 because shape data are lacking. Within any one kimberlite field, regardless of erosion level, kimberlite  
261 bodies vary in area over 2–3 orders of magnitude (Fig. 3)—typically 60–70% of the bodies are <10%



262 of the area of the largest pipe in the field. Those kimberlite fields inferred to have undergone a greater  
263 degree of erosion are composed of collectively smaller kimberlite bodies than the less-eroded fields  
264 (Fig. 3). This can be illustrated by plotting the area of the largest kimberlite pipe within a field against  
265 the estimated amount of erosion that each field has experienced (Fig. 5). The largest kimberlite bodies  
266 (<1500 m in diameter) are found in shallowly-eroded fields and may represent flared surface craters or  
267 coalesced neighboring pipes. Flaring of volcanic conduits in the near-surface is common (e.g., Keating  
268 et al., 2008; Ross et al., 2011; White and Ross, 2011) and can reflect: (1) more energetic explosions  
269 that disrupt more country rock at shallow depths compared to deeper explosions (Valentine and White,  
270 2012); (2) syn-eruptive collapse into the conduit of weak or poorly consolidated host rocks or  
271 neighboring kimberlite pipes; and (3) post-eruption collapse of crater walls (e.g., Pirrung et al., 2008).  
272 At 200–300 m erosion depths, non-flared kimberlite pipes have diameters up to ~500 m ( $8 \times 10^4 \text{ m}^2$ ),  
273 while those with flared craters (Orapa and Yubileina) are up to 900 m in diameter ( $6 \times 10^4 \text{ m}^2$ ). The  
274 diameters of the non-flared portions of the Orapa and Yubileina kimberlite pipes (~500 m depth)  
275 compare well with the maximum size of other kimberlite pipes at inferred equivalent depths (Fig. 5).  
276 At 500–800 m of inferred erosion levels (e.g., Venetia and Kimberley Group 1 fields, Table 1) the  
277 largest kimberlites are 300–400 m in diameter ( $8 \times 10^4$ – $1.2 \times 10^5 \text{ m}^2$ ), and at >1200 m erosion depths  
278 (Kimberley Group 2 field, Table 1) the largest kimberlite is only 260 m in diameter ( $5.5 \times 10^4 \text{ m}^2$ ).  
279 Acknowledging the uncertainties over paleo-depths from surface, the rate of decrease of maximum  
280 pipe sizes for erosion, from 1250 m (shallow) to 200 m (deep), is broadly consistent with pipe walls  
281 dipping inward at the typical observed slope angles of ~82–85° (equivalent to a 30 m decrease in  
282 diameter for every 100 m loss in height, Fig. 5).

283

## 284 **Review of physical geology of intraplate basaltic fields and their plumbing**

### 285 *Geologic settings, temporal patterns*

286 Basaltic volcanic fields occur in nearly all tectonic settings, including hot spot (e.g., Snake  
287 River Plain, U.S.A.; Kuntz et al., 1986), subduction zone (e.g., Michoacán-Guanajuato, México;  
288 Hasenaka and Carmichael, 1985), and back-arc (e.g., Ojikajima, Japan; Sudo et al., 1998). Here we  
289 focus on intraplate occurrences, which offer a closer analogy to the settings of most kimberlites.  
290 Intraplate basaltic fields occur far away from active plate margins on all continents and on the sea floor  
291 away from spreading centers (Hirano et al., 2006), and are dominated by monogenetic volcanoes.  
292 Fields typically are active for several millions of years: within many volcanic fields there are very  
293 young, well preserved volcanoes in proximity to eroded volcanoes, including those whose plumbing is

294 exposed, providing excellent opportunities to relate subsurface structure to eruptive processes and  
295 landforms (e.g., Hopi Buttes; White, 1991).

296 Most intraplate volcanic fields have alkali basalt affinities and are thought to represent low  
297 degrees of partial melting at depths of ~50–100 km. Some magmas appear to be sourced in lithospheric  
298 mantle, particularly early in a volcanic field's lifetime, while others have OIB compositions and some  
299 are ultramafic (e.g., minette, nephelenite, and other compositions). Mantle-derived xenoliths are  
300 common, but not ubiquitous. Many authors assume that this implies rapid ascent of the host magmas,  
301 but effusively-erupted lavas, as well as explosively erupted juvenile-rich pyroclastic deposits, contain  
302 mantle xenoliths and, therefore, their presence cannot imply explosive decompression from mantle  
303 depth as is sometimes inferred (e.g., McGetchin and Ullrich, 1973). Crustal xenoliths also occur in  
304 intraplate basalts but their abundance is strongly dependent upon whether eruptions are  
305 phreatomagmatic or magmatic (e.g., Valentine and Groves, 1996; Valentine, 2012).

306

### 307 *Spatial occurrences*

308 Like kimberlites, volcanoes in basaltic fields occur in a range of patterns from isolated to  
309 randomly distributed to fielded and aligned. Fields with tens or more volcanoes typically show some  
310 sort of fielding; a well-studied example is the Springerville field in Arizona, U.S.A. (Condit and  
311 Connor, 1996). The volcanoes in fields typically form over a span of time such that volcanic constructs  
312 overlap and bury each other where the vent density is very high, blurring the distinction between  
313 monogenetic and polygenetic activity. Conway et al. (1997) show how vent locations within fields can  
314 be closely associated with pre-existing, major crustal faults. Whether this association is simply a  
315 reflection of dikes preferentially ascending through weak zones in the crust, as is often assumed, or  
316 whether there is a link between crustal structure and deeper melt collection processes, is a question that  
317 remains open. Mazzarini and D'Orazio (2003) and Lesti et al. (2008) describe evidence of alignments  
318 and fields over ranges of length scales from hundreds of meters to tens of kilometers, and describe how  
319 these alignments relate to pre-existing crustal structure and to the thickness and mechanical properties  
320 of the lithosphere. At a local level, individual volcanoes, whether scattered or aligned with others, often  
321 occur along pre-existing faults (e.g., Hirano et al., 2006; Valentine and Krogh, 2006) that may not be  
322 oriented perpendicular to the least principal stress that normally controls dike orientation, although  
323 there are only limited conditions under which this process of "dike capture" can occur (Connor and  
324 Conway, 2000; Gaffney et al., 2007). Such relationships between pre-existing structure and vent  
325 location can be most pronounced in volcanic fields that have relatively low long-term magma fluxes  
326 (tectonically controlled fields; Valentine and Perry, 2007).

327  
328 *Dimensions of intraplate basaltic volcanoes and their plumbing structures*

329 Scoria cones

330 Scoria cones have typical basal diameters of ~400 m up to ~2.5 km (median value ~900 m;  
331 Wood, 1980), with summit craters that are typically ~40% as wide as the cone base (Wood, 1980). For  
332 our purposes, the measurement that is comparable to maar crater size is probably not the summit crater  
333 but the conduit or feeder dike width at the pre-eruptive surface, which is discussed below.

334 Keating et al. (2008) provide the only quantitative data that we are aware of on the shallow  
335 plumbing of small volume, intraplate basaltic volcanoes dominated by magmatic eruptions (e.g.,  
336 Strombolian, violent Strombolian, and Hawaiian). In the best constrained exposed plumbing systems  
337 that they described, vent structures are several tens of meters up to ~200 m wide at the paleo-surface,  
338 and the walls of the plumbing converge rapidly downward toward the feeder dike. The vent structures  
339 are much smaller than the typical footprint of the scoria cones that accumulate above them. The depth  
340 over which the vent structure transitions from its maximum width at the surface, to the feeder dike  
341 below, is also typically 10s of meters (in other words, the depth of the vent structure is similar to its  
342 diameter at the pre-eruptive surface, implying that vent complex margins dip inward ~60–70°). The  
343 feeder dikes observed by Keating et al. (2008) typically range between 1–10 m wide to depths of ~250  
344 m, and it is likely that they narrow below that depth because of increasingly limited interaction with the  
345 free surface. Indirect data based upon wall rock lithic contents from magmatic eruption products  
346 (Valentine and Groves, 1996; Valentine et al., 2007; Valentine, 2012) are consistent with volcano  
347 plumbing with widths on the order of ~tens of meters and less at depths <200 m. This can be  
348 complicated by widening produced by minor phreatomagmatic phases during an otherwise magmatic-  
349 dominated eruption. For example the Tolbachik scoria cone eruptions had brief phreatomagmatic  
350 phases that might have widened their plumbing by ~8–48 m at depths of >500 m (Doubik and Hill,  
351 1999), based upon the volume of erupted xenolith material, and assuming a 1600 m deep cylindrical  
352 conduit. It seems also reasonable that below a few hundred meters depth the plumbing geometry was  
353 that of a dike: the same xenolith volume could have been produced by only widening the dike by a few  
354 decimeters. To summarize, it appears that in most cases, the plumbing of monogenetic volcanoes  
355 dominated by magmatic eruptions is represented by relatively thin dikes at depths greater than ~200 m.  
356 Note that recent data (Geshi et al., 2010) suggest that the vent structures for small-volume basaltic  
357 eruptions can be much smaller, perhaps only a few meters wide at the pre-eruptive surface, although  
358 these data were measured on basaltic vents on a larger stratovolcano rather than an intraplate setting.  
359

360 Maars

361 Surprisingly few data compilations of maar crater sizes are available. Maar/tuff ring crater  
362 diameters for the examples in Table 2 range from 100-2000 m. Taddeucci et al. (2010) report maar  
363 diameters of 623–2536 m in the Alban Hills (Italy). Beget et al. (1996) document maars with diameters  
364 between 4000–8000 m, but these appear to be compound maars formed by the coalescence of multiple  
365 craters. Cas and Wright (1987) provide a histogram of crater diameters based upon data from 116  
366 maars. The distribution ranges from 200–3200 m with most craters between 400–1400 m and a mode  
367 of ~800 m. Unfortunately, the source data were never published, so it is not possible to reproduce the  
368 data or to understand the details of where and how the measurements were taken. Ross et al. (2011)  
369 provide crater depths and diameters for Quaternary maars, showing that the diameters range from  
370 ~100–1700 m, with most falling between 400–1200 m. It seems that ~400–1200 m is a reasonable  
371 representative diameter range for monogenetic maar and tuff ring craters.

372 White and Ross (2011) review diatremes formed beneath phreatomagmatic maar volcanoes, and  
373 compare them with kimberlite pipes. They conclude that the two types of features are similar in most of  
374 their physical characteristics. The phreatomagmatic diatreme literature includes some qualitative  
375 descriptions and diagrams of the vertical extent of diatremes (Lorenz, 1986; White, 1991; Martin and  
376 Németh, 2005; Auer et al., 2007; Lorenz and Kurszlaukis, 2007; McClintock et al., 2008) that give a  
377 sense of the vertical dimensions, but without any direct measurements due to the nature of exposures.  
378 Indirect data from wall rock lithic abundances support the general conclusion that diatremes for  
379 phreatomagmatic basaltic volcanoes extend 100s of meters to ~ 2 km depth (Lorenz, 1979; Valentine  
380 and Groves, 1996; Valentine, 2012), implying typical diatreme-country rock contacts dipping steeply  
381 inward from the surface crater diameters described above (White and Ross, 2011; also supported by  
382 limited geophysical data such as in Matthes et al., 2010). Diatremes can be less deep and with gentler  
383 dipping walls if host material is unconsolidated sediment and magma-water interaction is near or at the  
384 Earth's surface, (e.g., Ross et al., 2011; Blaikie et al., 2012). Most of the country rock disrupted by  
385 phreatomagmatic explosions remains within the diatreme, while only relatively shallow-seated  
386 explosions actually eject material out of the maar crater (strictly speaking, “shallow” is a relative term  
387 that depends upon explosion energy and should be referred to as “scaled depth;” e.g., Goto et al.,  
388 2001). Deep-seated country rock lithic clasts are mixed upward within the diatreme by subterranean  
389 explosions that may not directly erupt (debris jets, Ross and White, 2006; Ross et al., 2008a,b), and the  
390 lithic clasts are subsequently ejected onto the surface by shallow explosions (Valentine and White,  
391 2012), rather than being directly ejected from deep explosions as was suggested by Lorenz (1986).

392 Conversely, shallow-derived material, including tephra deposited on maar crater floors and material  
393 shed from collapsing crater walls, can be mixed downward by subsidence.

394

395 *Relative proportions of phreatomagmatic vs. magmatic volcano types in intraplate basaltic fields*

396 Intraplate, monogenetic basaltic volcanic fields are composed of varying combinations of scoria  
397 cones and their attendant lava fields, maars, small lava shields, and tuff rings and cones (the latter  
398 usually found where basalt erupted through standing surface water). Scoria cones, maars, and tuff rings  
399 are the most common vent-related landforms. Despite their abundance on the planet, there are  
400 surprisingly few well-documented data on the relative proportions of these dominant landforms. Table  
401 2 compiles data from fifteen volcanic fields for which we were able to find specific mention of the  
402 relative proportions of vent-related landforms. Eight of the volcanic fields contain 0–10% maars or tuff  
403 rings, the remaining vent-related landforms being dominated by scoria cones. It is worth noting that  
404 many of these are in arid or semi-arid climatic settings. The remaining four contain ~20–30% maars  
405 and tuff rings and are characterized by wetter climates, with the partially marine Auckland Volcanic  
406 Field potentially as high as 70% maars/tuff rings. The “footprints” of scoria cones are similar to the  
407 sizes of maar/tuff ring craters (see below), thus it is important to keep in mind that these proportions  
408 might underestimate the number of maars/tuff rings to some degree, because some volcanoes might  
409 have opening or early phreatomagmatic phases that later transition to magmatic activity which buries  
410 the early features in scoria, spatter, and/or lava (e.g., Lorenz and Büchel, 1980; White, 1991). The  
411 opposite can occur as well, where an eruption begins with scoria cone building that is later partly or  
412 wholly destroyed by phreatomagmatic maar forming activity (Gutmann, 2002). In two of the example  
413 volcanic fields in Table 2 (Southwest Nevada Volcanic Field, and Lunar Crater Volcanic Field), old  
414 and eroded vents, where early phreatomagmatic phases should crop out, do not indicate a significant  
415 number of “hidden” maars/tuff rings. Both of these volcanic fields reside in an arid region, and it is  
416 unclear whether this observation can be extended to volcanic fields in wetter settings.

417

418 *Dikes*

419 The magmas that feed intraplate monogenetic volcanoes ascend from their mantle sources via  
420 dikes, as do kimberlite magmas. The detailed structures within dikes associated with these volcanoes  
421 can show evidence for multiple pulses of magma (e.g., nested quenched margins and vesicle bands).  
422 This is especially true in the very shallow crust and where dikes extend within the volcanic constructs;  
423 Hintz and Valentine (2012) suggest that such pulsing reflects both variations in magma supply rate  
424 from depth, and shallow processes such as gas slugs ascending through volcanic plumbing (and

425 ultimately causing Strombolian bursts at the surface) and temporary vent blockage. Other dikes appear  
426 to have been emplaced in one event that had little temporal variation.

427         The dimensions of intraplate basaltic dikes are similar to those described for kimberlites. At  
428 shallow depths (~200 m or less), dikes can be several meters wide and locally wider where conduit  
429 structures have formed along them (Keating et al., 2008). Dike lengths at these depths range from  
430 hundreds of meters to a few kilometers (Valentine and Perry, 2006; Valentine and Keating, 2007). Sills  
431 can form at these shallow depths, especially along country rock bedding planes or where there are  
432 contrasts in rock properties (Kavanagh et al., 2006; Valentine and Krogh, 2006). Dikes exposed at  
433 deeper emplacement depths are notably thinner; Delaney and Gardner (1997) report a median dike  
434 width of 1.1 m (Utah, USA), which is inferred to be the feeder system of a deeply eroded (~400–2000  
435 m below paleo-surface) basaltic volcanic field. The same area has a median dike length of 1090 m,  
436 although in detail each dike crops out in many shorter segments (Delaney and Gardner, 1997).

#### 437 438 **Effects of landscape erosion on preservation of volcanic plumbing**

439         We now explore how a typical basaltic volcanic field might be represented in the geologic  
440 record of an area that undergoes progressive landscape erosion. Consider a volcanic field that, when  
441 active and un-eroded, has 90% scoria cones and 10% maars/tuff rings (Fig. 6), a reasonable scenario  
442 (Table 2). These proportions are based on a count of vent types. The relative area fractions presented  
443 by the two types of vent structures would be approximately equivalent to the proportions based upon a  
444 vent-type count in this young field because the footprints of scoria cones are similar in size to those of  
445 maars/tuff rings.

446         As the landscape erodes, pyroclastic deposits left by both magmatic and phreatomagmatic  
447 eruptions are removed relatively quickly, within a few Ma. Once the erosion level is generally close to  
448 the pre-eruptive surface, a geologic map would show areal proportions of volcanic features of ~50%  
449 scoria cone vent structures, and ~50% upper diatremes associated with maars and tuff rings. This  
450 reflects the difference in the scale of the upper plumbing of the vent types; even though the number of  
451 vent types remains the same, the scoria cone plumbing is about a factor of ten smaller (~100 m  
452 diameter) than the upper parts of diatremes (equivalent to the maar/tuff ring crater diameters—typically  
453 ~1000 m in diameter). When the landscape has been exhumed to ~100–200 m below the pre-eruptive  
454 surface, vent structures for most scoria cones will have completely merged into their feeder dikes,  
455 while diatremes associated with former maars/tuff rings might still have significant areal extent.  
456 Assuming that the feeder dikes average ~2 km in strike length and range between 2–5 m wide, a  
457 geologic map of the volcanic field once it has eroded to 300 m depth would have areal proportions of

458 volcanic (hypabyssal) features of ~80–90% diatreme material and ~10–20% feeder dikes (see Fig. 6).  
459 When erosion has stripped 1000 m, these areal proportions would comprise ~50–75% diatreme and  
460 ~25–50% feeder dike, because as the diatremes continue to narrow downward the dikes maintain a  
461 relatively constant geometry.

462 This is a hypothetical example showing that even if phreatomagmatic-dominated volcanoes are  
463 the minority in a volcanic field, landscape erosion will emphasize their plumbing structures compared  
464 to the more dominant magmatic-dominated structures. Other examples with different proportions of  
465 maars and scoria cones will have correspondingly different proportions of their respective plumbing  
466 features as the landscape erodes. However, it is clear that the differing physical scales of magmatic  
467 versus phreatomagmatic shallow plumbing result in an apparent predominance of phreatomagmatic  
468 features (diatremes) as a landscape is eroded.

469

#### 470 **Comparison of kimberlites and intraplate basaltic volcanic fields**

471 Our investigation of kimberlite and basaltic monogenetic fields indicates that they have more in  
472 common than they do have differences. The few kimberlite volcanoes that have been described (Igwise  
473 Hills volcanoes and the Fort à la Corne kimberlites) have surface dimensions that overlap with those of  
474 small monogenetic basaltic volcanoes (scoria cones, maars, and tuff rings and cones) and the eruptions  
475 that formed them were probably of similar magnitude to monogenetic basaltic eruptions. They provide  
476 little direct evidence for substantial subsurface diatremes and some may instead sit upon small volcanic  
477 conduits that transition into dikes at 200–300 m depth (e.g., Brown et al., 2012). They provide evidence  
478 that kimberlite magma can erupt in a variety of ways that are comparable to basaltic volcanism (e.g.,  
479 explosively, effusively and phreatomagmatically; e.g., Kjarsgaard et al., 2009).

480 The general subsurface plumbing systems (i.e., dikes versus diatremes) of both kimberlite and  
481 basaltic fields are similar, accounting for post-volcanic landscape erosion. We note that most published  
482 data on and interpretations of kimberlite volcanism are derived from studies of very large diamond-  
483 bearing kimberlite pipes that have been exposed by mining. These are mostly the largest ~5% of the  
484 ~900 kimberlite bodies used in this study. Our concern is that this could be equivalent to trying to  
485 describe monogenetic basaltic volcanism only from studies of eroded maar volcanoes whose craters  
486 exceed 1.5 km in diameter. Many smaller kimberlite bodies in kimberlite fields remain unstudied and  
487 comparisons between these and large mined kimberlite pipes are largely unexplored. Mining of many  
488 large kimberlite pipes reveals dikes and smaller pipes in the surrounding country rock and where  
489 kimberlite fields are well exposed dikes are abundant (e.g., Lesotho; Fig. 4 and Table 1). The ratio of  
490 dikes to pipes at different levels within kimberlite fields is not known. We suggest that the apparent

491 predominance of kimberlite pipes within fields in the geological record is at least partly a result of  
492 erosional bias due to removal of small and shallow volcanic structures and of the under reporting of  
493 kimberlite dikes due to their low economic importance and difficulty of geophysical detection. We  
494 suggest that kimberlite dikes may well be as common in kimberlite fields as they are beneath  
495 monogenetic basaltic fields.

496 The maximum size of a kimberlite pipe in a field appears to show a predictable relationship  
497 with erosion depth (at depths >200 m) equivalent to a structure with inward-dipping walls sloping at  
498 80–85° (Fig. 5). Acknowledging uncertainties over erosion depths, this may indicate that: A) it may be  
499 reasonable to use these slope angles to extrapolate deeply-eroded pipes upwards to within 100–200 m  
500 of the paleo-surface to estimate original dimensions; B) that there may be a maximum size that  
501 kimberlite pipes can grow to, probably due to a combination of dynamic (e.g., duration of eruption) and  
502 slope stability reasons (e.g., Sparks et al., 2006) and; C) that estimations of the erosion level of a region  
503 could be used to predict the maximum potential size of a kimberlite body expected in a newly  
504 identified field. By extrapolation, the 24% of kimberlite bodies that are <50 m diameter at <200 m  
505 depth in the Orapa field (Fig. 3) would have had surface crater diameters of <110 m (not accounting for  
506 any surface flaring) and would be less than 20 m wide at >300 m depth. Similarly, ~40% of kimberlite  
507 pipes in the Orapa field would have been <160 m wide at the surface and would be <10 m diameter at  
508 500 m depth. These extrapolated conduit dimensions are approaching the dimensions of those below  
509 scoria cones (e.g., Keating et al., 2008) and are comparable to the crater dimensions inferred below  
510 Holocene kimberlite scoria cones (Brown et al. 2012). This suggests to us that the Orapa kimberlite  
511 field may have contained small volcanoes which had little subsurface expression. In basaltic fields  
512 eroded to similar depths, subsurface diatremes typically account for between 0–30% of the feeder  
513 structures (the others being dikes; Table 2). Should a similar ratio hold true for kimberlites then the  
514 Orapa kimberlite field may have originally contained many more volcanoes, now lost through erosion.  
515 Thus some kimberlite fields may have had >400 volcanoes and, for example, if each eruption emitted  
516 0.001–0.01 km<sup>3</sup> of magma (typical volumes for monogenetic eruptions), then 0.4–40 km<sup>3</sup> of kimberlite  
517 magma could have made its way to the surface over the lifetime of a large kimberlite field.

518 That numerous kimberlite dikes are found at shallow levels in the crust (e.g., <300 m, Fig. 4) in  
519 some places indicates that kimberlite magma can rise to the near-surface without disintegrating into  
520 explosive flows that carve out wide and deep vents (pipes). This suggests that kimberlite magma may  
521 be commonly capable of feeding weakly explosive or effusive eruptions (e.g., Igwisi Hills volcanoes;  
522 Brown et al., 2012) in a manner typical of basaltic magmas. By analogy with intraplate, monogenetic  
523 basaltic volcanoes, the volume fluxes of these eruptions probably are <c. 10 m<sup>3</sup>/s. This begs the



524 question, why would some rising batches of kimberlite magma instead create deep pipes? In basaltic  
525 fields similar structures (diatremes) are generated by explosive interaction of magma with groundwater.  
526 A phreatomagmatic origin for kimberlite pipes has been proposed and elaborated (Lorenz, 1975;  
527 Lorenz and Kurszlaukis, 2007; White and Ross, 2011), but is not universally accepted, despite many  
528 similarities between diatremes constructed beneath maar volcanoes and kimberlite pipes. This is due in  
529 part to the unusual characteristics of kimberlite melts (e.g., very low silica contents, high CO<sub>2</sub> and H<sub>2</sub>O  
530 contents, inferred low magmatic viscosities and high degrees of mantle and crustal contamination;  
531 Mitchell 1986; Sparks et al. 2006), and resulting uncertainties over how they behave in the near-  
532 surface. High volatile contents are thought to enable kimberlite magmas to rise rapidly (Russell et al.,  
533 2012) and allow kimberlite magmas to erupt explosively and excavate wide, deep pipes (Sparks et al.,  
534 2006; Wilson and Head, 2007; Cas et al., 2008). Additionally, paleomagnetic studies of pyroclastic  
535 deposits within some kimberlite pipes indicate high (magmatic) emplacement temperatures (Fontana et  
536 al., 2011). An in-depth exploration of the behavior of volatiles in kimberlite melts is beyond the scope  
537 of this paper, but variations in the initial volatile loads or in the degassing history of successive  
538 batches of rising kimberlite magma could explain the variation in near-surface behavior, with volatile-  
539 rich batches erupting explosively and creating kimberlite pipes. However, a problem remains—if  
540 (volatile-poor) kimberlite magma can rise in dikes to the near-surface without excavating pipes, then  
541 what is to stop that magma interacting with groundwater to produce diatremes in a similar manner to  
542 basaltic magmas in near-surface dikes? In this case how might you distinguish a pipe created by a  
543 magmatic eruption from one created by a phreatomagmatic eruption? Some kimberlite pipes contain  
544 features indicative of magma-water interaction such as abundant accretionary lapilli (e.g., Porritt et al.,  
545 2009; Porritt and Russell, 2012), however these features are not universal in the deposits of basaltic  
546 maar volcanoes and their diagnostic value remains unclear.

547 A common counter argument against a phreatomagmatic model for kimberlite diatremes is that  
548 it would apparently require all kimberlites to erupt via phreatomagmatic mechanisms, implying in turn  
549 that all kimberlite magmas erupt to form pipes/diatremes (e.g., Sparks et al., 2006; Cas et al., 2008).  
550 With this perspective, the phreatomagmatic model seems like special pleading, since no other magma  
551 type on Earth has been observed to only erupt phreatomagmatically. This argument can be turned  
552 around: no other small volume, basic or ultrabasic magma type on Earth has been documented to form  
553 large diatremes via purely magmatic-volatile driven mechanisms, especially those of Plinian scale (as  
554 has been suggested for kimberlites, Sparks et al., 2006; Porritt et al., 2008). The material presented here  
555 suggests that it is probably not the case that all kimberlite eruptions form large diatremes, but rather  
556 that this perspective results from biases introduced by erosion of volcanic terrains, by site selection for

557 mining activity, and by underreporting of small features such as dikes. Our dataset and observations  
558 from numerous kimberlite fields suggests that kimberlite magmas erupt in a variety of ways. This is  
559 consistent with other magma types whose eruptive style is dependent on processes intrinsic to magma  
560 ascent (ascent speed, gas content, degassing history, and cooling rate) as well as environmental  
561 conditions (presence or absence of ground or surface water). In the absence of abundant data on the  
562 surface expression of kimberlite volcanoes with which to draw evidence on eruption style, we could  
563 benefit from looking to intraplate basaltic and ultramafic volcanic fields (e.g., Lake Natron-Engaruka  
564 monogenetic field, Mattsson and Tripoli, 2011; Hopi Buttes field, White, 1991). Despite differences in  
565 detail, such as the inferred high gas contents and low melt viscosities and of kimberlite magmas, there  
566 are many similarities with other more common volcanoes that can be explored.

567

## 568 **Conclusions**

569 The geological record, selective mining, and underreporting of dikes present a biased view of  
570 kimberlite volcanism. This bias is foremost a result of erosion that removes the products of eruptive  
571 activity that disrupts little country rock during ascent and leaves most of its record on the Earth's  
572 surface, and favors preservation of eruptions that disrupt large volumes of country rock and leave much  
573 of their record below the surface. We suggest that our current view of kimberlite volcanism is skewed  
574 by this bias and by the collection of most geological data from a very small sample composed of the  
575 largest known kimberlite pipes. There is a compelling correlation between the maximum size (area) of  
576 a kimberlite pipe in a field and the estimated amount of erosion that that field has experienced since  
577 emplacement that warrants further investigation. This may suggest that there is a maximum size that a  
578 kimberlite pipe can reach (~500 m diameter at ~200 m depth). The surface and subsurface expression  
579 and inferred eruptive products of kimberlite volcanism may be comparable in magnitude and dynamics  
580 to small monogenetic basaltic eruptions that are driven by magmatic, phreatomagmatic, and combined  
581 eruption mechanisms. In order to understand the full expression of kimberlite volcanism, we  
582 recommend that research efforts be turned towards the description and interpretation of small  
583 kimberlite bodies (e.g., dikes and small kimberlite pipes) as well as the shallow subsurface plumbing  
584 systems of other monogenetic mafic and ultrabasic volcanoes.

585

## 586 **Acknowledgements**

587 We thank Johann Stiefenhofer and Hielke Jelsma (De Beers), Shawn Harvey and George Read (Shore  
588 Gold Inc.), Wayne Pettit and Jon Carlson (BHP Billiton) and Don Duncan (Savannah Diamonds) for  
589 generously supplying proprietary data on kimberlite fields and for permission to publish. We thank

590 Claire Palmer for providing access to publications and for discussion. Lucy Porritt and Volker Lorenz  
591 are thanked for detailed helpful reviews and Michael Ort and Nancy Riggs are thanked for reviews and  
592 editorial stewardship. RJB thanks Matthew Field and Kelly Russell for their many useful discussions  
593 and comments. The ideas expressed in this paper are solely those of the authors.

594

## 595 **References**

596 Auer, A., Martin, U., Németh, K. 2007. The Fekete-hegy (Balaton Highland Hungary) “soft-substrate”  
597 and “hard-substrate” maar volcanoes in an aligned volcanic complex – Implications for vent geometry,  
598 subsurface stratigraphy and the paleoenvironmental setting. *J. Volcanol. Geotherm. Res.*, 159, 225–  
599 245.

600

601 Barnett, W.P., 2004. Subsidence breccias in kimberlite pipes- an application of fractal analysis. *Lithos*,  
602 76, 299–316.

603

604 Barnett, W.P., 2008. The rock mechanics of kimberlite volcanic pipe excavation. *J. Volcanol.*  
605 *Geotherm. Res.* 174, 29–39.

606

607 Basson, I.J., and Viola, G., 2003. Structural overview of selected Group II kimberlite dyke arrays in  
608 South Africa: implications for kimberlite emplacement mechanisms: *South African Journal of*  
609 *Geology*, 106, 375–394, doi: 10.2113/106.4.375.

610

611 Beget, J.E., Hopkins, D.M., Charron, S.D., 1996. The largest known maars on Earth, Seward  
612 Peninsula, northwest Alaska. *Arctic*, 49, 62–69.

613

614 Belousov, A.B., 2006. Distribution and eruption mechanism of maars in the Kamchatka Peninsula.  
615 *Doklady Earth Sci.*, 406, 24–27.

616

617 Berg, G.W., Carlson, J.A., 1998. The Leslie kimberlite pipe of Lac de Gras, Northwest Territories,  
618 Canada: Evidence for near surface hypabyssal emplacement. *Extended Abstracts 7th International*  
619 *Kimberlite Conference*, Cape Town, 81–83.

620

621 Berryman, A., Scott Smith, B.H., Jellicoe, B., 2004. Geology and diamond distribution of the 140/141  
622 kimberlite, Fort à la Corne, central Saskatchewan, Canada. *Lithos*, 76, 99–114.

623

624 Blaikie, T.N., Ailleres, L., Cas, R.A.F., Betts, P.G., 2012. Three-dimensional potential field modeling  
625 of a multi-vent maar-diatreme – The Lake Coragulac maar, Newer Volcanics Province, south-eastern  
626 Australia. *J. Volcanol. Geotherm. Res.*, 235–236, 70–83.

627

628 Brown, R.J., Kavanagh, J., Sparks, R.S.J., Tait, M., Field, M., 2007. Mechanically disrupted and  
629 chemically weakened zones in segmented dike systems cause vent localization: Evidence from  
630 kimberlite volcanic systems. *Geology* 35, 184–188.

631

632 Brown, R.J., Buse, B., Sparks, R.S.J., Field, M., 2008a. On the welding of pyroclasts from very low-  
633 viscosity magmas: Examples from kimberlite volcanoes. *J. Geol.* 116, 354–374.

634

635 Brown, R.J., Gernon, T., Stiefenhofer, J., Field, M., 2008b. Geological constraints on the eruption of  
636 the Jwaneng Central kimberlite pipe, Botswana. *J. Volcanol. Geotherm. Res.* 174, 195–208.

637

638 Brown, R.J., Tait, M., Field, M., Sparks, R.S.J., 2009. Geology of a complex kimberlite pipe (K2 pipe,  
639 Venetia mine, South Africa): Insights into conduit processes during explosive ultrabasic eruptions.  
640 *Bull. Volcanol.* 71, 95–112.

641

642 Brown, R.J., Many, S., Buisman, I., Field, M., Fontana, G., Mac Niocaill, C., Sparks, R.S.J., Stuart,  
643 F.N., 2012. Eruption of Kimberlite Magmas: Physical volcanology, Geomorphology, and Age of the  
644 Youngest Kimberlitic Volcanoes known on Earth (the Upper Pleistocene/Holocene Igwisi Hills  
645 volcanoes, Tanzania). *Bull. Volcanol.* 74, 1621–1643.

646

647 Carn, S., 2000. The Lamongan volcanic field, East Java, Indonesia: physical volcanology, historic  
648 activity and hazards. *J. Volcanol. Geotherm. Res.* 95, 81–108.

649

650 Cas, R.A.F., Wright, J.V., 1987. *Volcanic successions modern and ancient*. Allen & Unwin, London,  
651 487 pp.

652

653 Cas, R.A.F., Hayman, P., Pittari, A., Porritt, L., 2008. Some major problems with existing models and  
654 terminology associated with kimberlite pipes from a volcanological perspective, and some suggestions.  
655 *J. Volcanol. Geotherm. Res.* 174, 209–225.

656

657 Clement, C.R., 1982. A comparative geological study of some major kimberlite pipes in northern Cape  
658 and Orange Free State. PhD thesis (unpublished) University of Cape Town, pp 432.

659

660 Condit, C.D., Connor, C.B., 1996. Recurrence rates of volcanism in basaltic volcanic fields: An  
661 example from the Springerville volcanic field, Arizona: *Geol. Soc. Am. Bull.* 108, 1225–1241.

662

663 Connor, C.B., Conway, F.M., 2000. Basaltic volcanic fields. In: Sigurdsson, H. (Ed.), *Encyclopedia of*  
664 *Volcanoes*, Academic Press, New York, pp. 331–343.

665

666 Conway, F.M., Ferrill, D.A., Hall, C.M., Morris, A.P., Stamatakos, J.A., Connor, C.B., Halliday, A.N.,  
667 Condit, C., 1997. Timing of basaltic volcanism along the Mesa Butte Fault in the San Francisco  
668 Volcanic Field, Arizona, from  $^{40}\text{Ar}/^{39}\text{Ar}$  dates: Implications for longevity of cinder cone alignments. *J.*  
669 *Geophys. Res.* 102, 815–824.

670

671 Dawson, J.B., 1970. The structural setting of African kimberlite magmatism. In: Clifford, T.N., Gass,  
672 I.G. (Eds.), *African magmatism and tectonics*. Oliver and Boyd, Edinburgh, pp. 321–335.

673

674 Dawson, J.B., Hawthorne, J.B., 1973. Magmatic sedimentation and carbonatitic differentiation in  
675 kimberlite sills at Benfontein, South Africa. *J. Geol. Soc. London* 129, 61–85.

676

677 Dawson, J.B., 1994. Quaternary kimberlitic volcanism on the Tanzania craton. *Contrib. Min. Pet.* 116,  
678 473–485.

679

680 Delaney, P.T., Pollard, D.D., 1981. Deformation of host rocks and flow of magma during growth of  
681 Minette dikes and breccia-bearing intrusions near Ship Rock, New Mexico. *US Geol. Surv. Prof. Paper*  
682 1202, pp 60.

683

684 Delaney, P.T., Gartner, A.E., 1997. Physical processes of shallow mafic dike emplacement near the  
685 San Rafael Swell, Utah. *Geol. Soc. Am. Bull.* 109, 1177–1192.

686

687 Dempster, A.N., Tucker, R., 1973. The geology of the Sekameng (Buthe-Buthe) kimberlite pipe and  
688 the associated dyke swarm. In: Nixon, P.H., (Ed), 1973. Lesotho Kimberlites. Lesotho National  
689 Development Corporation, 180–189.

690

691 Doubik, P., Hill, B.E., 1999. Magmatic and hydromagmatic conduit development during the 1975  
692 Tolbachik eruption, Kamchatka, with implications for hazards assessment at Yucca Mountain, NV. *J.*  
693 *Volcanol. Geotherm. Res.* 91, 43-64.

694

695 Eley, R., Grütter, H., Louw, A., Tunguno, C., Twidale, J., 2008. Exploration Geology of the Luxinga  
696 Kimberlite Field (Angola) with Evidence Supporting the Presence of Kimberlite Lava. Extended  
697 Abstract, 9<sup>th</sup> Int. Kimberlite Conf., Frankfurt, Germany.

698

699 Field, M., Gibson, J.G., Wilkes, T.A., Gababotse, J., Khutjwe, P., 1997. The geology of the Orapa  
700 A/K1 Kimberlite, Botswana: further insight into the emplacement of kimberlite pipes. In: Dobretsov,  
701 N.L., Goldin, S.V., Kontorovich, A.E., Polyakov, G.V., Sobolev, N.V., (Eds), Proceedings of the Sixth  
702 International Kimberlite Conference, Novosibirsk, Russia: Kimberlites, Related Rocks and Mantle  
703 Xenoliths. *Russian Geology and Geophysics*, 38/1, 24–39.

704

705 Field, M., Scott Smith, B.H., 1999. Contrasting geology and near–surface emplacement of kimberlite  
706 pipes in southern Africa and Canada. In: Gurney, J., Gurney, J., Pascoe, M., Richardson, S. (Eds.),  
707 Dawson J.B. Proceedings of the VII International Kimberlite Conference. Vol. 1, Red Roof design cc,  
708 Cape Town, 214–237.

709

710 Field, M., Stiefenhofer, J., Robey, J., Kurszlaukis, S., 2008. The kimberlite–hosted diamond deposits of  
711 southern Africa: a review. *Ore Geol. Rev.*, 34, 33–75.

712

713 Fontana, G., Mac Nio Caill, C., Brown, R.J., Sparks, R.S.J., Field, M., 2011. Emplacement  
714 temperatures of pyroclastic and volcanoclastic deposits in kimberlite pipes in southern Africa. *Bull.*  
715 *Volcanol.*, 73, 1063–1083.

716

717 Gaffney, E.S., Damjanac, B., Valentine, G.A., 2007. Localization of volcanic activity: 2.Effects of pre-  
718 existing structure. *Earth Planet. Sci. Lett.* 263, 323-338, doi: 10.1016/j.epsl.2007.09.002.

719

720 Gernon, T., Sparks, R.S.J., Field, M., 2008. Degassing structures in volcanoclastic kimberlite: examples  
721 from southern African pipes. *J. Volcanol. Geotherm. Res.* 174, 186–194.  
722

723 Gernon, T.M., Fontana, G., Field, M., Sparks, R.S.J., Brown, R.J., Mac Niocaill, C., 2009a. Pyroclastic  
724 flow deposits from a kimberlite eruption: the Orapa south crater, Botswana. *Lithos*, 112, 566–578.  
725

726 Gernon, T.M., Fontana, G., Field, M., Sparks, R.S.J., 2009b. Depositional processes in a kimberlite  
727 crater: the Upper Cretaceous Orapa South Pipe (Botswana). *Sedimentology*, 56, 623–643.  
728

729 Gernon, T.M., Field, F., Sparks, R.S.J., 2012. Geology of the Snap Lake kimberlite intrusion,  
730 Northwest Territories, Canada: Field observations and their interpretation. *J. Geol. Soc.*, 169, 1–16.  
731

732 Geshi, N., Kusumoto, S., Gudmundsson, A., 2010. Geometric difference between non-feeder and  
733 feeder dikes. *Geology*, 38, 195–198, doi: 10.1130/G30350.1  
734

735 Goto, A., Taniguchi, H., Yoshida, M., Ohba, T., Oshima, H., 2001. Effects of explosion energy and  
736 depth to the formation of blast wave and crater: Field explosion experiment for the understanding of  
737 volcanic explosion. *Geophysic. Res. Lett.*, 28, 4287–4290.  
738

739 Gurney, J.J., Kirkley, M.B., 1996. Kimberlite dike mining in South Africa. *Spec. Ed. Africa Geosci.*,  
740 *Rev.*, 35–45.  
741

742 Gutmann, J.T., 2002. Strombolian and effusive activity as precursors to phreatomagmatism: eruptive  
743 sequence at maars of the Pinacate volcanic field, Sonora, Mexico. *J. Volcanol. Geotherm. Res.* 113,  
744 345–356.  
745

746 Haggerty, S.E., 1982. Kimberlites in Western Liberia: an overview of the geological setting in a plate  
747 tectonic framework. *J. Geophys. Res.* 87, 10811–10826.  
748

749 Hanson, E.K., Moore, J.M., Bordy, E.M., Marsh, J.S., Howarth, G., Robey, J.V.A., 2009. Cretaceous  
750 erosion in central South Africa: evidence from upper-crustal xenoliths in kimberlite diatremes. *South*  
751 *Africa J. Geol.* 112, 125–140.  
752

753 Hare, A.G., Cas, R.A.F., 2005. Volcanology and evolution of the Werribee Plains intraplate, basaltic  
754 lava flow-field, Newer Volcanics Province, southeast Australia. *Aus. J. Earth Sci.* 52, 59–78.  
755

756 Harvey, S., Kjarsgaard, B., McClintock, M., Shimell, M., Fourie, L., Du Plessis, P., Read, G., 2009.  
757 Geology and evaluation strategy of the Star and Orion South kimberlites, Fort à la Corne, Canada.  
758 *Lithos*, 112, 47–60  
759

760 Hasenaka.T., Carmichael, I.S.E., 1985. The cinder cones of Michoacan-Guanajuato, Central Mexico:  
761 their age, volume and distribution, and magma discharge rate. *J. Volcanol. Geotherm. Res.*, 25, 105–  
762 124.  
763

764 Hawthorne, J.B., 1975. Model of a kimberlite pipe. *Phys. Chem. Earth* 9, 1–15.  
765

766 Hintz, A.R., Valentine, G.A., 2012. Complex plumbing of monogenetic scoria cones: New insights  
767 from the Lunar Crater Volcanic Field (Nevada, USA). *J. Volcanol. Geotherm. Res.*, 239-240, 19–32.  
768

769 Hirano, N., Takahashi, E., Yamamoto, J., Abe, N., Ingle, S.P., Kaneoka, I., Hirata, T., Kimura, J.-I.,  
770 Ishii, T., Ogawa, Y., Machida, S., and Suyehiro, K., 2006. Volcanism in response to plate flexure:  
771 *Science*, 313, 1426–1428 and online supplemental material.  
772

773 Houghton, B.F., Wilson, C.J.N., Smith, I.E.M., 1999. Shallow-seated controls on styles of explosive  
774 basaltic volcanism: a case study from New Zealand. *J. Volcanol. Geotherm. Res.* 91, 97–120.  
775

776 Jelsma, H.A., de Wit, M.J., Thiart, C., Dirks, P.H.G.M., Viola, G., Basson, I.J., Anckar, E., 2004.  
777 Preferential distribution along transcontinental corridors of kimberlites and related rocks of southern  
778 Africa. *South African J. Geol.* 107, 301–324.  
779

780 Jelsma, H.A., de Wit, M.J., Thiart, C., Dirks, P.H.G.M., Viola, G., Basson, I.J., Anckar, E., 2004.  
781 Preferential distribution along transcontinental corridors of kimberlites and related rocks of southern  
782 Africa. *South African J. Geol.* 107, 301–324.  
783

784 Kavanagh, J.L., Menand, T., Sparks, R.S.J., 2006. An experimental investigation of sill formation and  
785 propagation in layered elastic media. *Earth Planet. Sci. Lett.*, 245, 799–813.



786

787 Kavanagh, J.L., Sparks, R.S.J., 2011. Insights of dyke emplacement mechanics from detailed 3D dyke  
788 thickness datasets. *J. Geol. Soc. London*, 168, 965–978.

789

790 Keating, G.N., Valentine, G.A., Krier, D.J., Perry, F.V., 2008. Shallow plumbing systems for small-  
791 volume basaltic volcanoes. *Bull. Volcanol.* 70, 563–582.

792

793 Kirkley, M.B., Kolebaba, M.R., Carlson, J.A., Gonzales, A.M., Dyck, D.R., Dierker, C., 1998.

794 Kimberlite emplacement processes interpreted from Lac de Gras examples. *Extended Abstracts*, 7<sup>th</sup>  
795 International Kimberlite Conference, Cape Town 429-431.

796

797 Kjarsgaard, B.A., 1996. Kimberlite-hosted diamond. In: Eckstrand, O.R., Sinclair, W.D., Thorpe, R.I.  
798 (Eds.), *Geology of Canadian Mineral Deposit Types*. *Geol. Surv. Canada*, 8, 560–568.

799

800 Kjarsgaard, B.A., 2007. Kimberlite diamond deposits. In: Goodfellow, W.D., Ed., *Mineral Deposits of*  
801 *Canada: A Synthesis of Major Deposit Types, District Metallogeny, the Evolution of Geological*  
802 *Provinces, and Exploration Methods: Geological Association of Canada, Mineral Deposits Division,*  
803 *Special Publication 5*, 245–272.

804

805 Kjarsgaard, B.A., Harvey, S., McClintock, M., Zonneveld, J.P., Du Plessis, P., McNeil, D., Heaman,  
806 L., 2009. *Geology of the Orion South kimberlite, Fort à la Corne, Canada*. *Lithos* 1125, 600–617.

807

808 Kresten, P., Dempster, A.N., 1973. The Geology of Pipe 200 and the Malibatso dyke swarm. In:  
809 Nixon, P.H., (Ed), 1973. *Lesotho Kimberlites*. *Lesotho National Development Corporation*, 172–179.

810

811 Kuntz, M.A., Champion, D.E., Spiker, E.C., LeFebvre, R.H., 1986. Contrasting magma types and  
812 steady-state, volume-predictable basaltic volcanism along the Great Rift, Idaho. *Geol. Soc. Am. Bull.*  
813 97, 579-594.

814

815 Kurszlaukis, S., Barnett, W.P., 2003. Volcanological and structural aspects of the Venetia Kimberlite  
816 field – a case study of South African kimberlite maar-diatreme volcanoes. *South African J. Earth Sci.*  
817 106, 165–192.

818

819 Kurszlaukis, S., Mahotkin, I., Rotman, A.Y., Kolesnikov, G.V., Makovchuk, I.V., 2009. Syn- and post-  
820 eruptive volcanic processes in the Yubileinaya kimberlite pipe, Yakutia, Russia, and implications for  
821 the emplacement of South African-style kimberlite pipes. *Lithos* 112, 579–591.  
822

823 Leckie, D.A., Kjarsgaard, B.A., Bloch, J., McIntyre, D., McNeil, D., Stasiuk, L., Heaman, L., 1997.  
824 Emplacement and reworking of Cretaceous, diamond-bearing, crater facies kimberlite of central  
825 Saskatchewan, Canada. *Geol. Soc. Am. Bull.* 109, 1000–1020.  
826

827 Lefebvre, N., Kurszlaukis, S., 2008. Contrasting eruption styles of the 147 Kimberlite, Fort à la Corne,  
828 Saskatchewan, Canada. *J. Volcanol. Geotherm. Res.*, 174, 171–185.  
829

830 Lesti, C., Giordano, G., Salvini, F., Cas, R.A.F., 2008. Volcano tectonic setting of the intraplate,  
831 Pliocene-Holocene, Newer Volcanic Province (southeast Australia): Role of crustal fracture zones. *J.*  
832 *Geophys. Res.* 113, B07407, doi:10.1029/2007JB005110.  
833

834 Lockhart, G., Grütter, H., Carlson, J., 2004. Temporal, geomagnetic and related attributes of kimberlite  
835 magmatism at Ekati, Northwest territories, Canada. *Lithos*, 77, 665–682.  
836

837 Lorenz, V., 1975. Formation of phreatomagmatic maar-diatreme volcanoes and its relevance to  
838 kimberlite diatremes. *Phys. Chem. Earth* 9, 17–27.  
839

840 Lorenz, V., 1979. Phreatomagmatic origin of the olivine melilitite diatremes of the Swabian Alb, Germany. In:  
841 Boyd, F.R. & Meyer, H.O.A. (Eds.): *Kimberlites, diatremes and diamonds: their geology, petrology and*  
842 *geochemistry. Proc. Sec. Int. Kimberlite Conf.*, 1, 354-363, Amer. Geophys. Union, Washington, USA.  
843

844 Lorenz, V., 1986. On the growth of maars and diatremes and its relevance to the formation of tuff  
845 rings. *Bull. Volcanol.*, 48, 265–290.  
846

847 Lorenz, V., Büchel, G., 1980. Zur Vulkanologie der Maare und Schlackenkegel der Westeifel.  
848 *Mitteilungen der Pollichia*, 68, 29–100.  
849

850 Lorenz, V., Kurszlaukis, S., 2007. Root zone processes in the phreatomagmatic pipe emplacement  
851 model and consequences for the evolution of maar-diatreme volcanoes. *J. Volcanol. Geotherm. Res.*  
852 159, 4–32.

853

854 Mainkar, D., Lehmann, B., Haggerty, S.E., 2004. The crater-facies kimberlite system of Tokapal,  
855 Bastar district, Chhattisgarh, India. *Lithos*, 76, 201–217.

856

857 Marsh, J., 1973. Relationships between transform directions and alkaline igneous rock lineaments in  
858 Africa and South America. *Earth Planet. Sci Lett.*, 18, 317–323.

859

860 Martin, U., Németh, K., 2005. Eruptive and depositional history of a Pliocene tuff ring that developed  
861 in a fluvio-lacustrine basin: Kissomlyó volcano (western Hungary). *J. Volcanol. Geotherm. Res.* 147,  
862 342–356.

863

864 Matthes, H., Kroner, C., Jahr, T., Kampf, H., 2010. Geophysical modeling of the Ebersbrunn diatreme,  
865 western Saxony, Germany. *Near Surface Geophys.*, 8, 311–319.

866

867 Mattsson, H.B., Tripoli, B.A., 2011. Depositional characteristics and volcanic landforms in the lake  
868 Natron-Engaruka monogenetic field, northern Tanzania. *J. Volcanol. Geotherm. Res.*, 203, 23–34.

869

870 Mazzarini, F., D’Orazio, M., 2003. Spatial distribution of cones and satellite-detected lineaments in the  
871 Pali Aike Volcanic Field (southernmost Patagonia): insights into the tectonic setting of a Neogene rift  
872 system. *J. Volcanol. Geotherm. Res.* 125, 291–305.

873

874 McClintock, M., White, J.D.L., Houghton, B.F., Skilling, I.P., 2008. Physical volcanology of a large  
875 crater-complex formed during the initial stages of Karoo flood basalt volcanism, Sterkspruit, Eastern  
876 Cape, South Africa. *J. Volcanol. Geotherm. Res.* 172, 93–111.

877

878 McGetchin, T.R., Ullrich, G.W., 1973. Xenoliths in maars and diatremes with inferences for the  
879 Moon, Mars, and Venus. *J. Geophys. Res.* 78, 1833–1853.

880

881 Mitchell, R.H., 1986. *Kimberlites. Mineralogy, Geochemistry and Petrology.* Plenum Press 442 p.

882

883 Moore, A., Blenkinsop, T., Cotterill, F., 2008. Controls on post-Gondwana alkaline volcanism in  
884 Southern Africa. *Earth Planet. Sci. Lett.* 268, 151–164.  
885

886 Moss, S., Russell, J.K., Brett, R.C., Andrews, G.D.M., 2009. Spatial and temporal evolution of  
887 kimberlite magma at A154N, Diavik, Northwest Territories, Canada. *Lithos*, 112, 541–552.  
888

889 Nixon, P.H., 1973. How wide, how long, what shape? The vital statistics of Lesotho kimberlites.  
890 Unpublished report: Department of mines and geology, Lesotho, PHN/16.  
891

892 Nixon, P.H., 1995. The morphology and nature of primary diamondiferous occurrences. *J. Geochem.*  
893 *Ex.* 53, 41–71.  
894

895 Nowicki, T., Crawford, B., Dyck, D., Carlson, J., McElroy, R., Oshust, P., Helmstaedt, H., 2004. The  
896 geology of kimberlite pipes of the Ekati property, Northwest Territories, Canada. *Lithos* 76, 1–27.  
897

898 Pettit, W., 2009. Geophysical signatures of some recently discovered large (N40 ha) kimberlite pipes  
899 on the Alto Cuilo concession in north-eastern Angola. *J. Volcanol. Geotherm. Res.*, 112:106–115.  
900

901 Pirrung, M., Büchel, G., Lorenz, V., Treutler, H., 2008. Post-eruptive development of the Ukinrek  
902 east maar since its eruption in 1977 A.D. in the periglacial area of south-west Alaska. *Sedimentology*  
903 55, 305–334.  
904

905 Pittari, A., Cas, R.A.F., Lefebvre, N., Robey, J., Kurszlaukis, S., Webb, K. 2008. Eruption processes  
906 and facies architecture of the Orion Central kimberlite volcanic complex, Fort à la Corne,  
907 Saskatchewan; kimberlite mass flow deposits in a sedimentary basin. *J. Volcanol. Geotherm. Res.*, 174,  
908 152–170.  
909

910 Porritt, L.A., Cas, R.A.F., Crawford, B., 2008. In-vent column collapse as an alternative model for  
911 massive volcanoclastic kimberlite emplacement: An example from the Fox kimberlite, Ekati Diamond  
912 Mine, NWT, Canada. *J. Volcanol. Geotherm. Res.*, 174, 90–102.  
913

914 Porritt, L.A., Cas, R.A.F., 2009. Reconstruction of a kimberlite eruption, using an integrated  
915 volcanological, geochemical and numerical approach: A case study of the Fox Kimberlite, NWT,  
916 Canada. *J. Volcanol. Geotherm. Res.* 179, 241–264.  
917

918 Porritt, L.A., Russell, J.K., 2012. Kimberlite ash: fact or fiction? *Phys. Chem. Earth*, 45–46, 24–32.  
919

920 Robles-Cruz, S.E., Watangua, M., Isidoro, L., Melgarejo, J.C., Galí, S., Olimpio, A., 2009. Contrasting  
921 compositions and textures of ilmenite in the Catoca kimberlite, Angola, and implications in exploration  
922 for diamond. *Lithos*, 112, 966–975.  
923

924 Rolfe, D.G., 1973. The geology of the Kao kimberlites. In: Nixon, P.H., 1973. *Lesotho Kimberlites*,  
925 Lesotho National Development Corporation, 101-105.  
926

927 Rombouts, L., 1987. Geology and evaluation of the Guinean diamond deposits. *Annales de la Société*  
928 *Géologique de Belgique*, 110, 241–259.  
929

930 Ross, P.-S., White, J.D.L., 2006. Debris jets in continental phreatomagmatic volcanoes: A field study  
931 on their subterranean deposits in the Coombs Hill vent complex, Antarctica: *J. Volcanol. Geotherm.*  
932 *Res.*, 149, 62–84.  
933

934 Ross, P.-S., White, J.D.L., Zimanowski, B., Büttner, R., 2008a. Multiphase flow above explosion sites  
935 in debris-filled volcanic vents: Insights from analogue experiments: *J. Volcanol. Geotherm. Res.*, 178,  
936 104–112.  
937

938 Ross, P.-S., White, J.D.L., Zimanowski, B., Büttner, R., 2008b. Rapid injection of particles and gas  
939 into non-fluidized granular material, and some volcanological implications. *Bull. Volcanol.*, 70, 1151–  
940 1168, doi: 10.1007/s00445-008-0230-1.  
941

942 Ross, P.-S., Delpit, S., Haller, M.J., Németh, K., Corbella, H., 2011. Influence of the substrate on maar-  
943 diatreme volcanoes—an example of a mixed setting from the Pali Aike volcanic field, Argentina. *J.*  
944 *Volcanol. Geotherm. Res.* 201, 253–271.  
945

946 Russell, J.K., Porritt, L.A., Lavallee, Y., Dingwell, D.B., 2012. Kimberlite ascent by assimilation-  
947 fuelled buoyancy. *Nature*, 481, 352–356.

948

949 Schmincke, H-U., 2007. The Quaternary volcanic fields of the East and West Eifel (Germany). In:  
950 Ritter, R., Christensen, U., (Eds) *Mantle plumes-a multidisciplinary approach*. Springer-Heidelberg, pp  
951 241.

952

953 Skinner, E.M.W., Marsh, J.S., 2004. Distinct kimberlite pipe classes with contrasting eruption  
954 processes. *Lithos* 76, 183–200.

955

956 Smith, E.I., Sánchez, A., Walker, J., Wang, K., 1999. Geochemistry of mafic magmas in the Hurricane  
957 volcanic field, Utah: Implications for small- and large-scale chemical variability of the lithospheric  
958 mantle: *J. Geol.*, 107, 433–448.

959

960 Smith, I.E.M., Blake, S., Wilson, C.J.N., Houghton, B.J., 2008. Deep-seated fractionation during the  
961 rise of a small-volume basalt magma batch: Crater Hill, Auckland, New Zealand. *Contrib. Mineral.*  
962 *Petrol.* 155, 511–527.

963

964 Snyder, D.B., Lockhart, G.D., 2005. Kimberlite trends in NW Canada. *J. Geol. Soc. London*, 162, 737–  
965 740.

966

967 Sottili, G., Palladino, D.M., Gaeta, M., Masotta, M., 2012. Origins and energetics of maar volcanoes:  
968 examples from the ultrapotassic Sabatini Volcanic District (Roman Province, Central Italy). *Bull.*  
969 *Volcanol.*, 74. 163–186. doi: 10.1007/s00445-011-0506-8.

970

971 Sparks, R.S.J., Baker, L., Brown, R.J., Field, M., Schumacher, J., Stripp, G., 2006. Dynamical  
972 constraints on kimberlite volcanism. *J. Volcanol. Geotherm. Res.* 155, 18–48.

973

974 Stiefenhofer, J., Farrow, D.J., 2004. Geology of the Mwadui kimberlite, Shinyanga district, Tanzania.  
975 *Lithos*, 76, 139–160.

976

977 Sudo, M., Uto, K., Tatsumi, Y., Matsui, K., 1998. K-Ar geochronology of a Quaternary monogenetic  
978 volcano group in Ojika Jima District, Southwest Japan. *Bull. Volcanol.* 60, 171–186.

979

980 Taddeucci, J., Sottili, G., Palladino, D.M., Ventura, G., Scarlato, P., 2010. A note on maar eruption  
981 energetics: current models and their application. *Bull. Volcanol.* 72, 75–83, doi:10.1007/s00445-009-  
982 0298-2.

983

984 Valentine, G.A., 2012. Shallow plumbing systems for small-volume basaltic volcanoes, 2: Evidence  
985 from crustal xenoliths at scoria cones and maars. *J. Volcanol. Geotherm. Res.*, 223–224, 47–63,  
986 doi:10.1016/j.jvolgeores.2012.01.012.

987

988 Valentine, G.A., Groves, K.R., 1996. Entrainment of country rock during basaltic eruptions of the  
989 Lucero volcanic field, New Mexico. *J. Geol.*, 104, 71–90.

990

991 Valentine, G.A., Krogh, K.E.C., 2006. Emplacement of shallow dikes and sills beneath a small basaltic  
992 volcanic center – The role of pre-existing structure (Paiute Ridge, southern Nevada, USA). *Earth  
993 Planet. Sci Letts.* 246, 217–230.

994

995 Valentine, G.A., Perry, F.V., 2006. Decreasing magmatic footprints of individual volcanoes in a  
996 waning basaltic field. *Geophys. Res. Lett.* 33, L14305.doi:10.1029/2006GL026743.

997

998 Valentine, G.A., Keating, G.N., 2007. Eruptive styles and inferences about plumbing systems at  
999 Hidden Cone and Little Black Peak scoria cone volcanoes (Nevada, U.S.A.). *Bull. Volcanol.*, 70, 104–  
1000 113. doi:10.1007/s00445-007-0123-8.

1001

1002 Valentine, G.A., Perry, F.V., 2007. Tectonically controlled, time-predictable basaltic volcanism from a  
1003 lithospheric mantle source (central Basin and Range Province, USA). *Earth Planet. Sci. Lett.*, 261,  
1004 201–216. doi:10.1016/j.epsl.2007.06.029.

1005

1006 Valentine, G.A., White, J.D.L., 2012. Revised conceptual model for maar-diatremes: subsurface  
1007 processes, energetics, and eruptive products. *Geology*, doi: 10.1130/G33411.1.

1008

1009 Valentine, G.A., Krier, D.J., Perry, F.V., Heiken, G., 2007. Eruptive and geomorphic processes at the  
1010 Lathrop Wells scoria cone volcano. *J. Volcanol. Geotherm. Res.*, 161, 57–80.  
1011 doi:10.1016/j.jvolgeores.2006.11.003.

1012  
1013 Valentine, G.A., Shufelt, N.L., Hintz, A.R.L., 2011. Models of maar volcanoes, Lunar Crater (Nevada,  
1014 USA). *Bull. Volcanol.* 73, 753–765, doi: 10.1007/s00445.011-0451-6.  
1015  
1016 Vearncombe, S., Vearncombe, J.R., 2002. Tectonic controls on kimberlite location, South Africa. *J.*  
1017 *Structural Geol.* 24, 1619–1625.  
1018  
1019 Walters, A.L., Phillips, J.C., Brown, R.J., Field, M., Gernon, T., Stripp, G., 2006. The role of  
1020 fluidisation in the formation of volcanoclastic kimberlite: Grain size observations and experimental  
1021 investigation. *J. Volcanol. Geotherm. Res.* 155, 119–137.  
1022  
1023 Webb, K.J., Scott Smith, B.H., Paul, J.L., Hetman, C.M., 2004. Geology of the Victor Kimberlite,  
1024 Attawapiskat, Northern Ontario, Canada: cross-cutting and nested craters. *Lithos*, 76, 29–50.  
1025  
1026 White, J.D.L., 1991. Maar-diatreme phreatomagmatism at Hopi Buttes, Navajo Nation (Arizona),  
1027 USA. *Bull. Volcanol.* 53, 239–258.  
1028  
1029 White, J.D.L., Ross, P-S., 2011. Maar-diatreme volcanoes: A review. *J. Volcanol. Geotherm. Res.* 201,  
1030 1–29.  
1031  
1032 White, J.L., Sparks, R.S.J., Bailey, K., Barnett, W.P., Field, M., Windsor, L., 2012. Kimberlite sills and  
1033 dikes associated with the Wesselton kimberlite pipe, Kimberley, South Africa. *South African J. Geol.*  
1034 115, 1–32.  
1035  
1036 White, S.H., de Boorder, H., Smith, C.B., 1995. Structural controls of kimberlite and lamproite  
1037 emplacement. *J. Geochem. Exp.* 53, 245–264.  
1038  
1039 Wilson, L., Head, J.W. III., 2007. An integrated model of kimberlite ascent and eruption. *Nature*, 447,  
1040 53–57.  
1041  
1042 Wood, C.A., 1980. Morphometric evolution of cinder cones. *J. Volcanol. Geotherm. Res.* 7, 387–413.  
1043



1044 Zonneveld, J-P., Kjarsgaard, B.A., Harvey, S.E., Heaman, L.M., McNeil, D.H., Marcia, K.Y., 2004.  
1045 Sedimentologic and stratigraphic constraints on the emplacement of the Star kimberlite east-central  
1046 Saskatchewan. *Lithos*, 76, 115–138.

1047

1048

1049 **Figure captions**

1050

1051 **Figure 1.** Small volcanic cones of the Holocene Igwisi Hills volcanoes, Tanzania (modified from  
1052 Brown et al., 2012). Surface crater diameters are <100–200 m.

1053

1054 **Figure 2.** The Fort à la Corne kimberlite field. The kimberlite field comprises pyroclastic cones and  
1055 craters and is buried beneath glacial till. Larger bodies represent coalesced kimberlite deposits from  
1056 two or more kimberlite volcanoes (courtesy of S. Harvey, Shore Gold Inc.).

1057

1058 **Figure 3.** Histograms and cumulative frequency curves of the areas of ~500 kimberlites from four  
1059 kimberlite fields exposed at various erosion levels.

1060

1061 **Figure 4.** Kimberlite dikes and pipes in northern Lesotho (from Jelsma et al., 2009). Estimated erosion  
1062 level is 300 m below paleo-surface (Hanson et al. 2009). Kimberlite pipes are circled.

1063

1064 **Figure 5.** Plot of the size of the maximum pipe in a kimberlite field against the estimated erosion level  
1065 of that field. Pipes to the right of the vertical dashed line may represent flared craters and/or two or  
1066 more coalesced bodies. Red arrow indicates dimensions of non-flared parts of the Orapa south and  
1067 Yubileina pipes. There is a reasonably consistent decrease in maximum pipe size with erosion depth  
1068 >200 m. This is comparable to that of a pipe with average wall slopes of ~80–85°. Margins of error for  
1069 the amount of erosion are not well constrained and may vary from <100 m to >200 m. Grey symbols  
1070 relate to pipes for which there is little geological evidence for erosion levels. The data suggest that the  
1071 maximum diameter of a kimberlite pipe at around 200 m below the surface is ~500 m. At shallower  
1072 depths the diameter of a pipe is dependent on flaring, which is controlled by proximity to neighboring  
1073 pipes, the thickness of poorly consolidated surface rocks or sediments, and for surface deposits, the  
1074 coalescence of neighboring edifices. Diameters are calculated from the diameter of equivalent area  
1075 circle. <sup>1</sup>Pettit (2009); <sup>2</sup>pers comm. Shoregold Diamonds; <sup>3</sup>Stiefenhofer and Farrow, (2004); <sup>4</sup>reported in  
1076 Robles-Cruz et al., 2009; <sup>5</sup>Field et al., 1997; <sup>6</sup>Nowicki et al. (2004); <sup>7</sup>Brown et al., (2009); <sup>8</sup>Kurszlaukis

1077 et al., (2009); <sup>9</sup>De Beers internal report; <sup>10</sup>Rolfe (1973); <sup>11</sup>De Beers internal report; <sup>12</sup>Kurszlaukis and  
1078 Barnett, (2003); <sup>13</sup>Webb et al., (2004); <sup>14</sup>De Beers internal report; <sup>15</sup>Rombouts (1987). \*erosion  
1079 estimates from Hanson et al., (2009).

1080

1081 **Figure 6.** Cartoon illustrating the effects of landscape erosion on the preserved record of monogenetic  
1082 basaltic volcanism. A) Map and cross-section of a basaltic volcanic field comprised of scoria cones and  
1083 maar volcanoes. The surface is dominated by the products of effusive and weakly explosive eruptions  
1084 (scoria cones and lavas). B) Following 100–200 m of erosion, the vent structures of scoria cones have  
1085 merged down into their feeder dikes, while the diatreme still has significant area extent. This results in  
1086 an apparent predominance of phreatomagmatic features (diatremes) as the landscape is eroded.

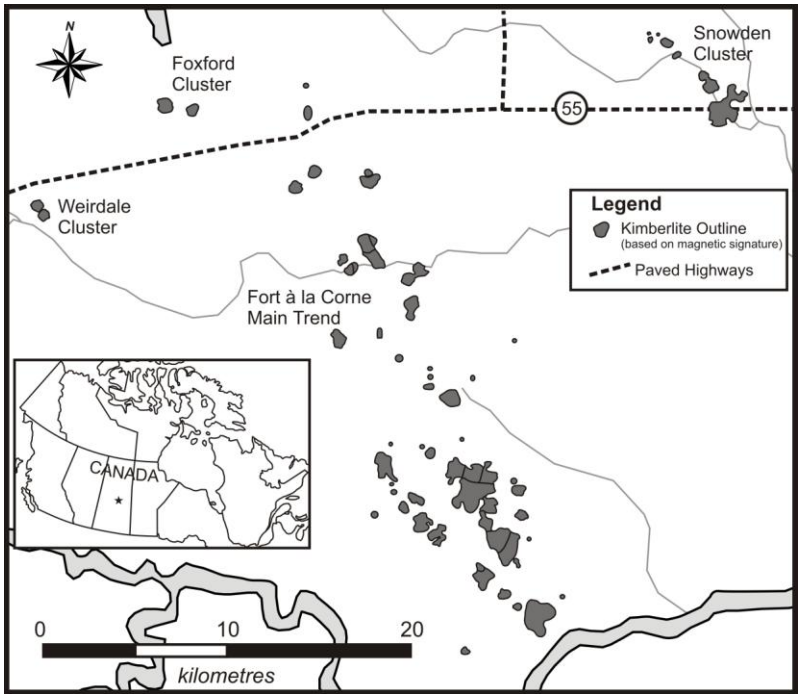
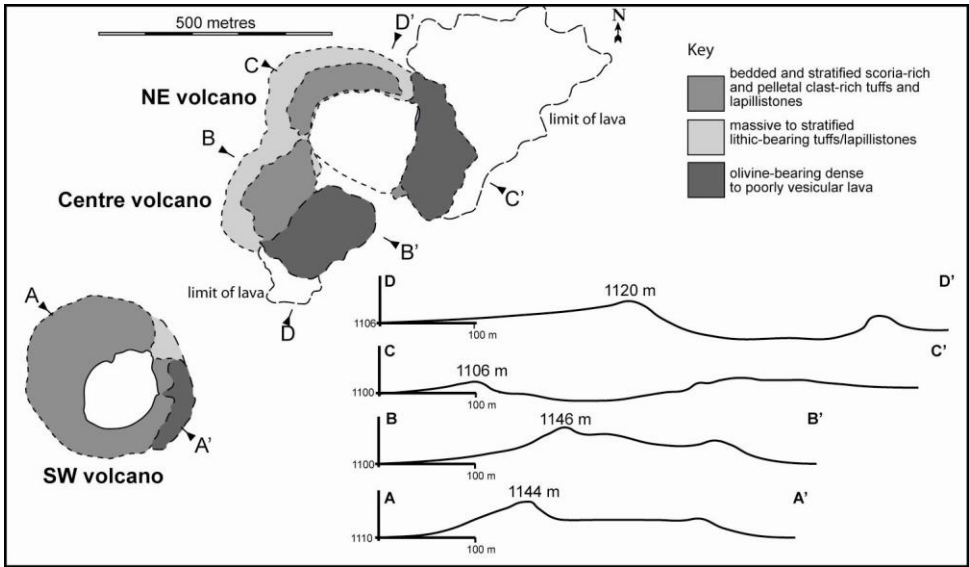
Kimberlite field	<sup>1</sup> Age (Ma)	Overburden	Estimated erosion level (m)	No. of pipes	Size range (10 <sup>4</sup> m <sup>2</sup> )	<sup>2</sup> d pipe (m)	No. of dikes	Country rock geology	Comments	Sources of data/references
Alto Cuilo, Angola	146–111	Kalahari sand	0	205	0.5–174	80–1500	-	Erupted into poorly consolidated to unconsolidated sediment	-	BHP Billiton data; Pettit (2009); Eley et al. (2008)
Fort à la Corne, Canada	106–98	Glacial deposits ~ 100 m thick	0	69	4–403 [largest single body = 139]	220–2300 [1350]	-	Marine sediments	Surface kimberlite volcanoes; some coalesced.	Shore Gold data: Berryman et al. (2004); Zonneveld et al., (2004)
Tanzania	189; 53	?	?<100	113	1–146	110–1360	present	? Basement	Poorly constrained dataset	Savannah Diamonds data
Orapa, Botswana	90	Kalahari sand	<<200	85	0.1–66	35–900	Present; not reported	Karoo basalt; sedimentary cover at time of eruption	-	De Beers data; Field et al. (1997); Gernon et al. (2009b)
Jwaneng, Botswana	240	Kalahari sand	<250	15	0.1–54	35–830	Present, not reported	Karoo basalt; sedimentary cover at time of eruption	-	De Beers data; Specific examples: Brown et al. (2008b)
Lesotho	Cretaceous	No	<300*	17	0.4–20	70–500	220; 21 blows	Karoo basalt lava	Exposed in mountainous highlands	Nixon (1973)
Ekati-Lac de Gras, Canada	75–43	Glacial deposits	<<500	159	0.1–16	30–450	Present (>13)	Archean metasediments and granitoids; Cretaceous Tertiary strata present at time of eruption	-	BHP Billiton data; Berg and Carlson, (1998); Carlson et al, (1998); Kirkley et al, (1998); Nowicki et al, (2004); Lockhart et al, (2004)
Kgare, Botswana	80	?Kalahari sand	<500	13	0.3–8	60–300	-	-	-	De Beers data
Venetia, South Africa	520	No	~500	15	0.1–12.5	35–400	>4	Metamorphic basement; sedimentary and volcanic rock cover.	15 kimberlite bodies in 4 km <sup>2</sup>	Kurszlaukis and Barnett(2003); Brown et al. (2009)
Kimberley Group 1, South Africa	111–87	No	850*	68	0.1–12.7	35–400	Present; not reported	Metamorphic basement; sedimentary and volcanic rock cover	-	De Beers data; summary in Field et al. (2008)
Guinea	95	?	1000	19	0.1–9.5	35–340	Numerous	Metamorphic basement	-	Rombouts (1987)

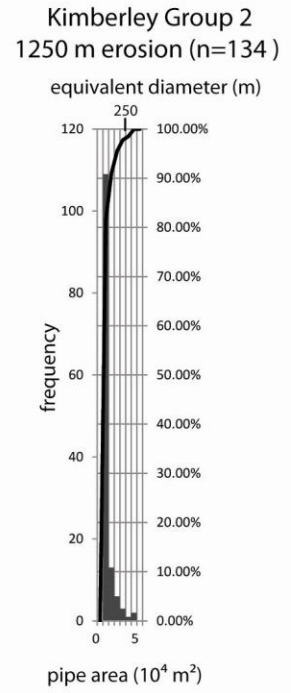
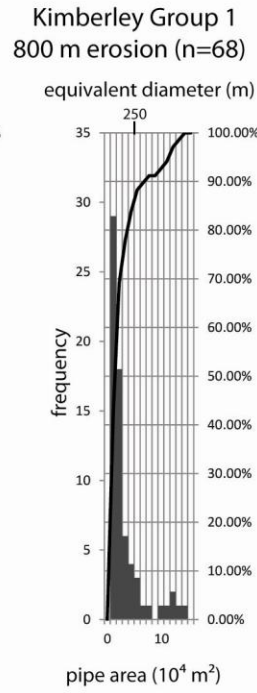
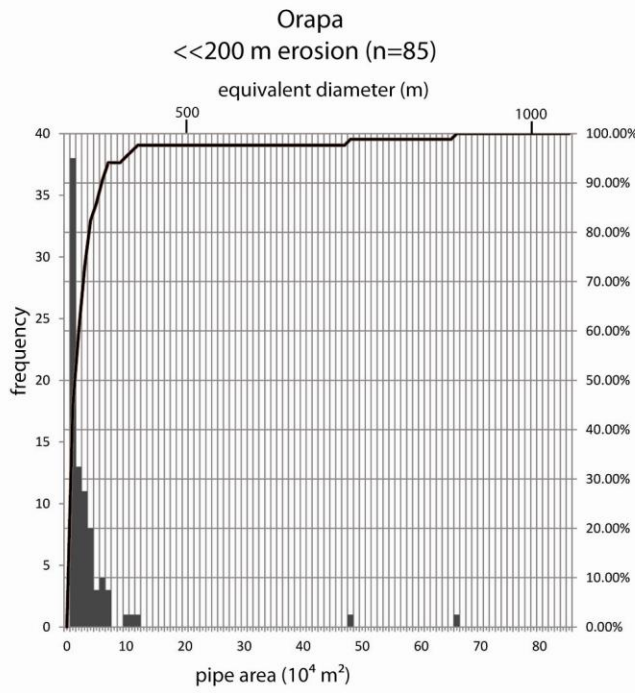
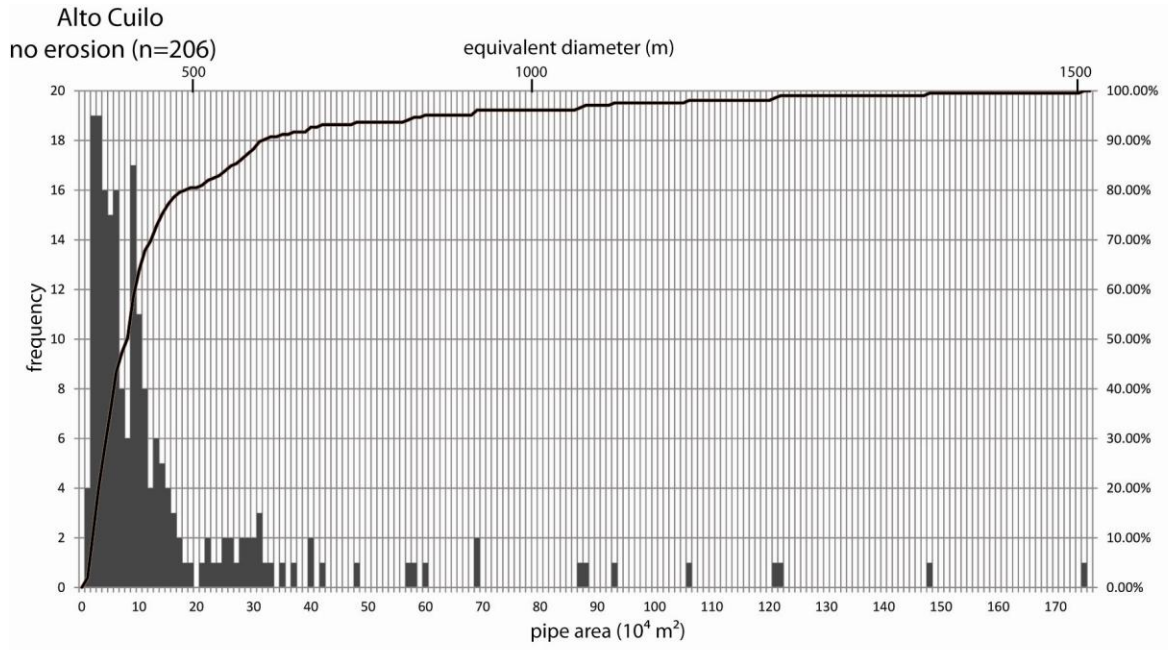
Kimberley Group 2, South Africa	119–114	No	1250*	134	0.06–5.5	26–260	Present; not reported	Metamorphic basement; sedimentary and volcanic rock cover	-	De Beers data; summary in Field et al. (2008)
---------------------------------------	---------	----	-------	-----	----------	--------	-----------------------------	---	---	--

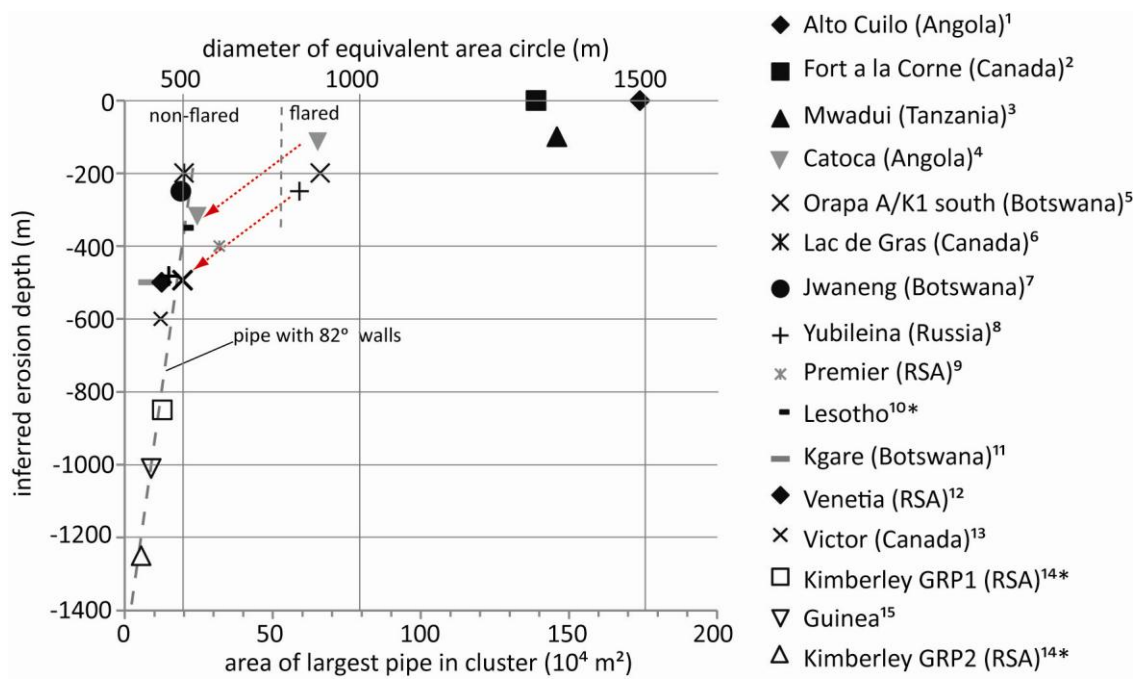
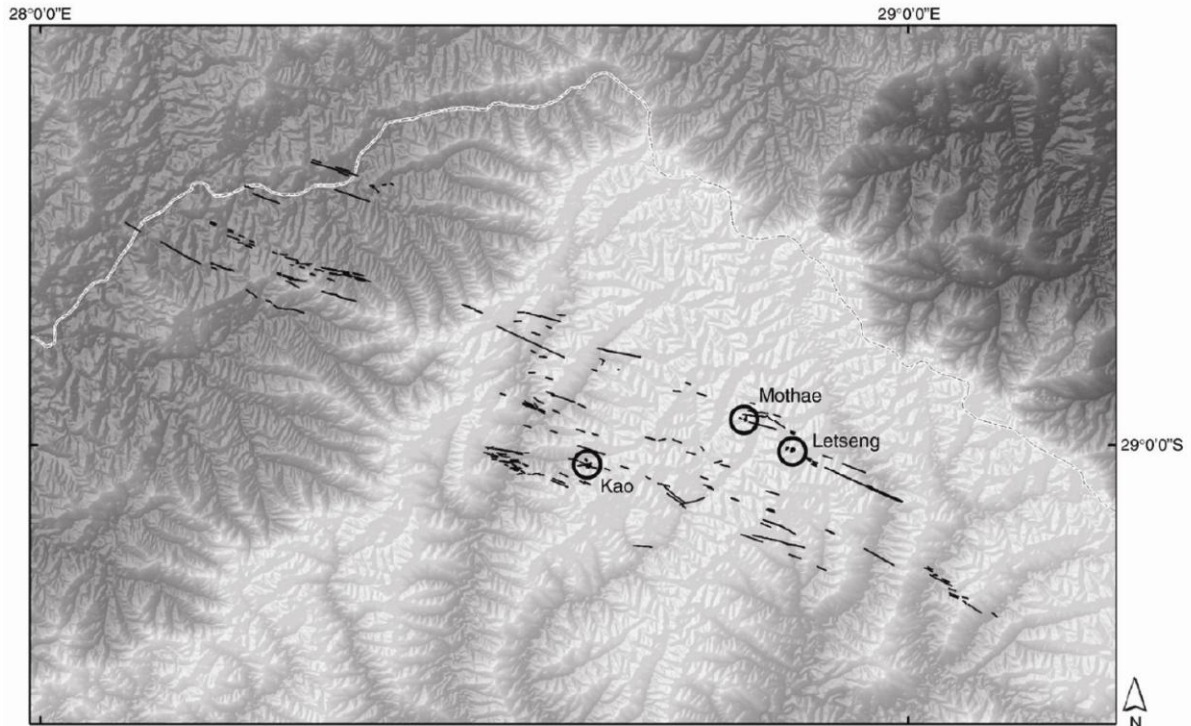
**Table 1.** Summary of data on kimberlite fields used in this study. <sup>1</sup>not all kimberlites in a field have been dated. <sup>2</sup>diameters of equivalent area circle.\*erosion estimates from Hanson et al., (2009).

Volcanic field	Total volcanoes	% maars or tuff rings	Maar and tuff ring crater sizes	Reference
West Eifel, Germany	~240	30%	< 1700 m	Schmincke H-U (2007)
East Eifel, Germany	~100	“rare”		Schmincke H-U (2007)
Lamongan, East Java, Indonesia	~90	32%	100–800 m, “typical” ~450 m	Carn (2000)
Seward Peninsula, AK, USA	No data	No data	4000–8000 m	Beget et al. (1996)
Michoacan-Guanajuato, Mexico	1040 (43 domes, 13 shields, 22 maars/tuff rings)	2%	Not documented	Hasenaka and Carmichael (1985)
Springerville, AZ, USA	409 (5 maars, 4 fissure vents, 2 shields, several spatter mounds)	1%	Not documented	Condit and Connor (1996)
Newer Volcanic Province, Victoria, Australia	~400 (~50% scoria cones, 40% shields, 10% maars/tuff rings)	10%	1000–2000 m average diameter	Hare and Cas (2005)
Pali Aike volcanic field, Patagonia (Argentina-Chile)	139 (34 maars, remainder scoria cones)	24%	Crater diameter not provided	Mazzarini and D’Orazio (2003) – note we combined their U2 and U3 chronologic units
Pinacate volcanic field, Sonora, Mexico	400 scoria cones, 8 maars	2%	800–1600 m for 5 maars for which data are provided	Gutmann (2002)
Auckland volcanic field, New Zealand	49 basaltic centers		34 are “principally phreatomagmatic”	Houghton et al. (1999)
Hurricane volcanic field, Utah, USA	10 basaltic centers	0	All scoria cones	Smith et al. (1999)
Southwest Nevada volcanic field (Plio-Pleistocene), NV, USA	17 basaltic centers (6 buried)	0 (out of 11 exposed volcanoes)	Scoria cones and one shield	Valentine and Perry (2007)
Lunar Crater volcanic field, NV, USA	>100 basaltic centers	<5% (four likely ones in Pleistocene, plus perhaps two in older Pliocene volcanoes)		Valentine et al. (2011)
Sabatini volcanic district, Italy	45 (14 maars, remainder scoria cones)	31%	600–1700 m	Sottili et al. (2012)
Kamchatka peninsula, Russia	?>3000 (~34 maars, the rest scoria cones)	<1%	200–1600 m	Belousov (2006)

Table 2. Sizes and proportions of phreatomagmatic maars in basaltic volcanic field.



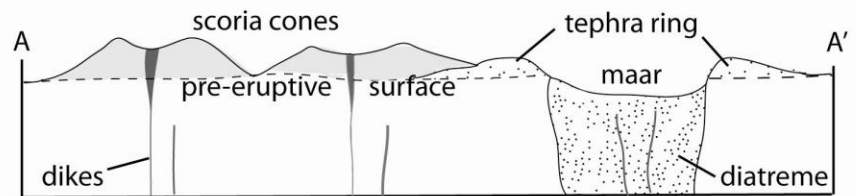
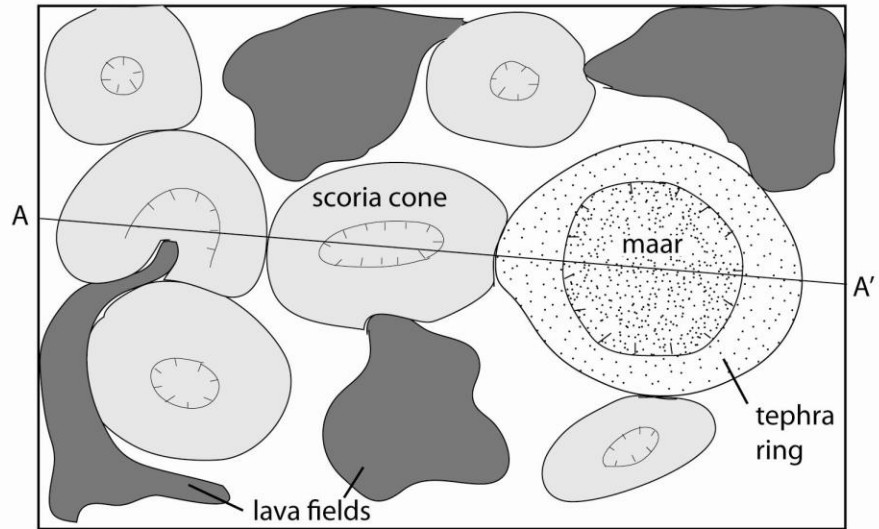






**A**

Map view

**B**

Map view

